I&EC research
Industrial & Engineering Chemistry Research

Process Systems Engineering

A sequential integration between optimal flexible heat exchanger network synthesis and control structure design

Lautaro Braccia, Pablo Andres Marchetti, Patricio A. Luppi, and David Alejandro R. Zumoffen

Ind. Eng. Chem. Res., **Just Accepted Manuscript** • DOI: 10.1021/acs.iecr.8b01611 • Publication Date (Web): 11 Jul 2018

ACS Publications

is published by the American Chemical Society. 1155 Sixteenth Street N.W., Washington, DC 20036

A sequential integration between optimal flexible heat exchanger network synthesis and control structure design

Lautaro Braccia,*,† Pablo A. Marchetti,‡ Patricio Luppi,†,¶ and David Zumoffen†,§

†*Grupo de Ingeniería de Sistemas de Procesos (GISP), Centro Franco-Argentino de Ciencias de la Información y de Sistemas (CIFASIS), CONICET-UNR, 27 de Febrero 210 bis, (S2000EZP) Rosario, Argentina.*

‡*Instituto de Desarrollo Tecnológico para la Industria Química (INTEC), UNL-CONICET, Güemes 3450, (3000) Santa Fe, Argentina.*

¶*Universidad Nacional de Rosario, Rosario, Argentina*

§*Universidad Tecnológica Nacional – FRRo, Rosario, Argentina*

E-mail: braccia@cifasis-conicet.gov.ar

Phone: +54-341-4237248 int. 332. Fax: +54-341-482-1772

Abstract

In this work, the optimal synthesis and control structure design (CSD) problems for flexible heat exchanger networks (HENs) are integrated into a new sequential methodology. The proposed approach relies, on the one hand, on a convexification and outer-approximation strategy to solve the synthesis stage and, on the other hand, on the sum of squared deviations (SSD) method for the optimal CSD. These methods guarantee the optimality of the synthesis process as well as the proper operation of the HEN in

several operating points. The first stage of the proposed approach, which focuses on the flexible HEN synthesis problem, considers both temperature and flow rate modifications in the inlet streams. A multi-period synthesis formulation is proposed where critical points are iteratively incorporated to fulfill the flexibility requirements. Because the problem size and the non-convexities increase when additional critical points are considered, both the convexification of nonlinear terms and an outer approximation strategy are used to guarantee the optimality of the solutions at this stage. The second stage handles the decisions associated to the design of the control structure. This stage is critical because the network is required to work in a wide range of operating points. If the classical CSD method based on the well-know relative gain array (RGA) is applied, and only the nominal operating point is considered, such requirement is not fullfiled. In fact, this work demonstrates that such classical CSD approach is not enough to operate the HEN in the range of variation considered by the multi-period synthesis phase. As an alternative method, the application of the SSD approach to multiple operating points is proposed. Thus, several optimal control structures are developed to ensure the operability of the HEN. Three academic case studies are presented to illustrate the application of the proposed methodology.

1 Introduction

Being an important component of any process, energy recovery through heat exchanger networks (HENs) is one of the most studied problems in Chemical Engineering. Moreover, HEN configuration and the interaction of these networks with the rest of the process can impose strong control limitations due to competitive effects, inverse response, and time delays. A correct design of such energy integration directly impacts not only the feasibility but also the final profit of the overall plant [1].

The conventional methods for synthesizing HENs assume fixed operating parameters at nominal conditions and are based on either sequential or simultaneous approaches. Sequen-

tial synthesis methods aim to reduce the computational burden at this stage by dividing the overall problem into a series of subproblems. Relevant publications in this category are Papoulias and Grossmann[2], Linnhoff and Hindmarsh[3], and Floudas et al.[4]. In contrast, simultaneous methods do not decompose the problem but address the capital and operational costs in a trade-off fashion. One of the most referenced simultaneous models has been proposed by Yee and Grossmann[5], where a stage-superstructure representation (the Synheat model) is formulated using a mixed-integer nonlinear programming (MINLP) approach. Several contributions extending this framework appear in the literature. Ponce-Ortega et al.[6] and Grossmann et al.[7] include isothermal streams with phase change into the synthesis model. Onishi et al.[8], Serna-Gonzalez et al.[9], Mizutani et al.[10], and Frausto-Hernandez et al.[11] also extended the Synheat model incorporating detailed equipment design and fluid dynamic considerations such as pressure drop. A review of proposed methodologies to synthesize HENs can be found in the work of Furman and Sahinidis[12].

The simultaneous synthesis formulations are, in general, very hard to solve due to the presence of non-convex expressions and binary decision variables. In some cases current state-of-the-art solvers not only fail to obtain the global optimal solutions but also fail to obtain a feasible solution. Therefore, alternative global optimization methods have been proposed to solve this kind of problems. For instance, several works presented algorithmic alternatives that ensure global convergence of the Synheat model. Björk and Westerlund[13] and Braccia et al.[14] proposed global optimization approaches which apply convexification of signomial terms to guarantee global convergence and optimality. An outer optimization algorithm for a MINLP model involving concave and bilinear terms has been developed by Bergamini et al.[15]. In turn, Zamora and Grossmann[16] proposed a thermodynamic-based convex underestimation of the HEN synthesis problem, which is implemented through a branch-and-bound algorithm. Also, Adjiman et al.[17] solve the problem using the αBB-algorithm and assuming a linear cost-function for the involved area. All these works use the Synheat model as their basis.

The consideration of potential disturbance changes, which are always present in any type of industrial process, is another important aspect to be taken into account. Disturbances play a significant role because they affect both the economic performance and the operational specifications of the whole process. Hence, the design of HENs requires to account for flexibility considerations. In this context, Aaltola[18], Chen and Hung[19], Verheyen and Zhang[20], and Escobar et al.[21] present multi-period formulations based on the Synheat model to handle the synthesis of flexible HENs (Synflex). While the Synheat model is used to design the network at the nominal operating point, the Synflex model takes into account different periods/scenarios which allow to consider several disturbances in the network. Thus, the main goal of the flexible synthesis problem is to find an optimal network configuration that operates within a specified range of expected disturbances, e.g., changes in temperatures and flow rates of the inlet streams.

Because several periods are considered, the flexible approach increases the size and complexity of the formulation with respect to the basic Synheat model. However, from the literature review it can be concluded that global optimization strategies have not been applied to the Synflex formulation, which is an important gap to be covered.

At the process control level, several approaches were proposed in the literature during the last decades. The control structure design (CSD) problem depends on the selected HEN structure[22] and, therefore, the analysis of controllability should be considered as an integral part of network design. Calandranis and Stephanopoulos[23] introduced an approach that ensures structural controllability of a HEN. In their work, both the design and operation problems are addressed. While the first problem decides the configuration of the control loop, the second problem sequences the control actions of the loop to accommodate set-point changes and reject load disturbances. In turn, Aguilera and Marchetti[24] developed a procedure for the on-line optimization and control system design of a HEN using an MINLP approach. Besides, the dynamic resilience and a heuristic method to decide the bypass placement of HENs have been studied in Mathisen et al.[25] and Mathisen et al.[26],

respectively. Later, a systematic framework for the synthesis and retrofit of flexible and structurally controllable HENs has been presented by Papalexandri and Pistikopoulos[27,28]. More recently, Yang et al.[29] introduced a unified model to quantify disturbance propagations in a HEN. Based on the latter, a design procedure to handle optimal bypass selection is presented in Yang et al.[30]. Moreover, a sequential procedure for flexible HEN synthesis and control structure design has been proposed by Escobar et al.[21]. They use the classical relative gain array (RGA) methodology at nominal operating point to define the best decentralized control structure. This task is performed off-line by evaluating several control structures obtained from different input combinations. Finally, Braccia et al.[31] introduced a flexible HEN synthesis method integrated with the design technique of a fully-decentralized reconfigurable control structure (CS) given by Luppi et al.[32]. The advantage of this method is that it provides alternative control structures able to act at different operating points. The design is made using steady-state process information only.

It is important to recall that heat exchange networks are always embedded in some particular industrial process. In this sense, if we analyze the inlet disturbances of a HEN, these disturbances are generally caused by operational changes in some process units. Similarly, the output variables of the network are, in general, inlet streams of downstream process units which must be kept on a given reference value. For this reason, since the HEN should be considered in the context of the overall process, it is important to perform the synthesis taking into account flexibility considerations and a control structure design that is capable of rejecting the expected disturbances.

1.1 Contribution of this work

In this work a new sequential optimization methodology to synthesize flexible HENs with optimal control structure is presented. The new methodology allows, on the one hand, solving the multi-period flexible synthesis stage while guaranteeing the quality of the solution and, on the other hand, designing an optimal control structure which handles multiple operating

points by applying the sum of squared deviations (SSD) procedure.

The main contributions of the proposed method are the following:

- An optimization strategy based on both convexification and outer-approximation is proposed to solve the synthesis stage, therefore guaranteeing the quality of the solution. In contrast, the works presented by Aaltola[18], Chen and Hung[19], Verheyen and Zhang[20], and Escobar et al.[21] do not guarantee that the solution found is optimal.

- This work illustrates how local optimization methods can obtain a local solution for the Synflex problem when the size of the problem or the number of periods being considered increases. This behavior has been previously reported only by Björk and Westerlund[13] for the Synheat problem.

- The proposed methodology allows designing the HEN control structure to be operable within a given range of expected disturbances. In contrast, most of previous contributions design the control structure at the nominal operating point, e.g. Escobar et al.[21] and Yang et al.[30].

- The complete solution methodology, including both synthesis and control structure design problems, is implemented with the same modelling tool (i.e., the GAMS environment). This systematic treatment of the problem contrastes with the heuristic off-line screening and stochastic global search methods proposed by Escobar et al.[21] and Braccia et al.[31], respectively.

- The proposed formulation sets the foundations for future simultaneous methodologies integrating process control and process synthesis and design.

This paper is organized as follows: this introduction section has been presented to contextualize the problem on hand and give an overview of the classical and flexible approaches to HEN synthesis, the associated optimization strategies, and the control structure design problem. The inherent drawbacks of the alternative methodologies have also been presented.

Section 2 outlines the sequential methodology proposed in this work. The main concepts regarding flexible HEN synthesis are presented in Section 2.1. In particular, a more detailed discussion of the multi-period synthesis model and the flexibility index is presented in Sections 2.1.1 and 2.1.2, respectively. The proposed optimization strategy, required to obtain the model solutions, is introduced in Section 2.2. Sections 2.2.1 and 2.2.2 discuss the approach in detail. The main concepts and specific implementation issues related to the SSD subproblem for control structure design (CSD) are discussed in Section 2.3. A detailed algorithmic description of the proposed method is given in Section 2.4. The application of the proposed approach to several examples from the literature is presented in Sections 3.1, 3.2, and 3.3. Finally, Section 4 summarizes the conclusions, discussion, and future work.

2 Proposed Sequential Methodology

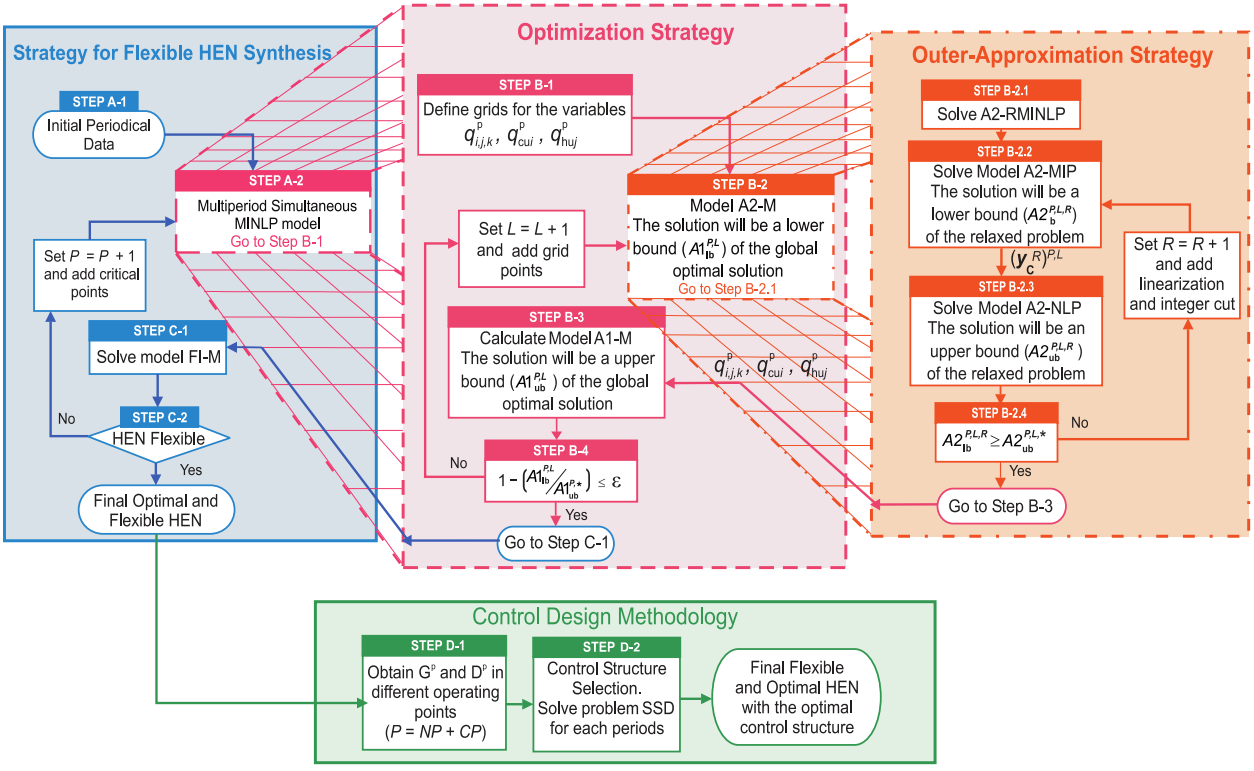

Figure 1: Proposed flexible HEN synthesis and optimal control structure design scheme

The proposed methodology sequentially addressing the flexible HEN synthesis and control

structure design problems is summarized in Figure 1. Both a multi-period formulation and a flexibility index model, which are iteratively evaluated, are used to solve the flexible HEN synthesis problem. Multiple operating conditions are considered besides the nominal operating point. In order to simplify the computational burden, the flexibility requirement is not directly taken into account in the multi-period synthesis formulation. The aim of the flexible synthesis stage is to obtain a network design able to operable within an expected range of disturbances (such as changes of the flow rates and temperatures) for the inlet process streams.

A sequence of multi-period HEN synthesis and flexibility problems is solved. As the number of periods increases, the number of continuous and binary variables of the multi-period formulation substantially grows and a poor solution can be obtained. To guarantee convergence and improve the performance of the algorithm, an iterative strategy combining convexification and convex mixed-integer optimization is used[13]. Each multi-period formulation (referred as A1-M) is modified using convexification of signomial terms to obtain an approximate model (named A2-M). In the latter, an initial set of grid points is proposed for the approximation of each non-convex term. An iterative procedure is applied where, at each step, the current approximate model A2-M is solved and its solution is used as fixed values to evaluate the non-convex terms and objective function of the original formulation A1-M. The objective values obtained for the approximate and original models are lower and upper bounds, respectively, of the multi-period formulation being tackled. Through successive iterations, which introduce additional grid points to the convexified model, a better approximation of the original formulation together with a more accurate solution are obtained. In order to solve the models A2-M the outer approximation technique presented in Viswanathan and Grossmann[33] is used. The convexification applied to the approximate model guarantees the latter technique to obtain the global optimum.

Once an optimal and flexible HEN is obtained, an appropriate control structure able to handle its operation is designed. To guarantee a proper operation of the HEN within the

expected disturbance variation range, the SSD subproblem (referred as model SSD-M) is solved for each period. Hence, at each operating point a decentralized control structure is obtained. A detailed description of the formulations A1-M, A2-M, and SSD-M, together with the required sets and variables, is given in the next sections.

2.1 Flexible Heat Exchanger Network Synthesis

The flexible HEN synthesis problem is formulated using a multiscenario/multiperiod optimization model in which a finite number of periods is considered to handle the uncertainty. The problem is solved using an iterative procedure consisting of two-stages[18–21]. In the first stage, a multi-period HEN problem is solved to obtain both the design and the operation variables. In the second stage, the flexibility problem is solved in order to find the flexibility index of the current network and a new critical point. At the first iteration (represented with $P = 1$), only one operating point (the nominal point) is considered, being the multi-period formulation equivalent to a single-period formulation, i.e. the Synheat model of Yee and Grossmann[5]. At each iteration $P \geq 2$, the critical point obtained from the previous flexibility problem is incorporated as a new period (scenario) in the multi-period formulation to increase the flexibility of the network. The procedure is stopped when the designed HEN is able to operate satisfactorily over the entire desired disturbance range.

2.1.1 Multi-period Heat Exchanger Networks Synthesis

The multi-period network synthesis problem is formulated as a superstructure-based multiperiod MINLP model with $k \in K = \{1, \ldots, \mathrm{N_T}\}$ stages where the matching for heat exchange between $i \in I = \{1, \ldots, \mathrm{N_H}\}$ hot and $j \in J = \{1, \ldots, \mathrm{N_C}\}$ cold streams is selected. The network needs to support inlet flow disturbances such as those of temperature and flow rate. The general structure of the model, referred as A1-M, is shown in eq. (1). This problem involves the binary variables $\mathbf{y}_\mathrm{H}$ representing the existence and operation, respectively, of heat exchangers and utility exchangers, and the continuous variables $\mathbf{x}_\mathrm{H}$ denoting stream

temperatures, exchanged heat, approach temperatures, and exchange areas. In this model, the superscript/subscript $p \in \mathbb{N}$ represents each operating point (or period). At each iteration (P) of the synthesis strategy a new critical point is added and, therefore, the total number of periods is increased by one. For this reason, $p = 1$ means the nominal point and $p > 1$ means any other operating condition (i.e., the nominal operating point and additional critical points are considering at each iteration $P > 1$). For a detailed description of the model, see the Supporting Information File.

Problem A1-M:

$$A1^P = \min_{\mathbf{x}_H, \mathbf{y}_H} \ \mathbf{c_f y} + \mathbf{c_d d} + \sum_{p=1}^{P} C(\mathbf{z}_p) \tag{1a}$$

$$\text{s.t.} \quad \mathbf{A y} + \mathbf{B y}'_p + \mathbf{h}(\mathbf{x}_p, \mathbf{z}_p, \mathbf{d}, \boldsymbol{\theta}_p) = 0, \tag{1b}$$

$$\mathbf{C y} + \mathbf{D y}'_p + \mathbf{f}(\mathbf{x}_p, \mathbf{z}_p, \mathbf{d}, \boldsymbol{\theta}_p) \leq 0, \tag{1c}$$

$$\mathbf{g}(\mathbf{x}_p, \mathbf{z}_p, \mathbf{d}, \boldsymbol{\theta}_p) \leq 0, \tag{1d}$$

$$\mathbf{x}_p^{LO} \leq \mathbf{x}_p \leq \mathbf{x}_p^{UP}, \quad \mathbf{x}_p \in \mathbb{R}^n \tag{1e}$$

$$\mathbf{z}_p^{LO} \leq \mathbf{z}_p \leq \mathbf{z}_p^{UP}, \quad \mathbf{z}_p \in \mathbb{R}^q \tag{1f}$$

$$\mathbf{d}^{LO} \leq \mathbf{d} \leq \mathbf{d}^{UP}, \quad \mathbf{d} \in \mathbb{R}^q \tag{1g}$$

$$\mathbf{y} \in \{0,1\}^q, \quad \mathbf{y}'_p \in \{0,1\}^q \tag{1h}$$

$$\forall p = 1, \ldots, P \tag{1i}$$

$$\mathbf{x}_H = \langle \mathbf{x}_p, \mathbf{z}_p, \mathbf{d} \rangle, \quad \mathbf{y}_H = \langle \mathbf{y}, \mathbf{y}'_p \rangle$$

In eq. (1), $A1^P$ represents the optimal value of the economic objective function for the final HEN at iteration P, where P operating points $(\boldsymbol{\theta}_1, \boldsymbol{\theta}_2, \ldots, \boldsymbol{\theta}_P)$ are considered. The vectors of independent (manipulated) variables (e.g., heat flow for heat exchangers and utility exchangers) and dependent (state) variables are denoted $\mathbf{z}_p \in \mathbb{R}^q$ and $\mathbf{x}_p \in \mathbb{R}^n$, respectively, where $q = [\mathrm{N_H} \times \mathrm{N_C} \times \mathrm{N_T} + \mathrm{N_H} + \mathrm{N_C}]$ and $n = [q + \mathrm{N_H} \times \mathrm{N_T} + \mathrm{N_C} \times \mathrm{N_T}]$. The design variables (area of heat exchangers and utility exchangers) are represented by $\mathbf{d}$. In turn, the uncertain

parameters at period p, which can change during the operation (i.e., inlet temperatures and flowrates), are given by $\boldsymbol{\theta}_p$. The binary variables $\mathbf{y}$ and $\mathbf{y}'_p$ represent the existence and operation at p, respectively, of heat exchangers and utility exchangers. The non-linear terms of the set of equality and inequality constrains are defined using the vector functions $\mathbf{h}$ and $\mathbf{f}$, respectively. Moreover, the set of correlations associated to the estimation of the design variables is determined by the function $\mathbf{g}$. On the one hand, notice that the state variables ($\mathbf{x}_p$), manipulated variables ($\mathbf{z}_p$), and operation binary variables ($\mathbf{y}'_p$), all depend on the number of periods being considered in the model. This dependency is represented by the subscript p. On the other hand, the design variables, $\mathbf{d}$, and the existence of heat exchangers and utility exchangers, $\mathbf{y}$, do not depend on the number of periods. The objective function is the total annual cost (TAC), where the first term represents a fixed cost associated to the selected heat exchangers, the second term is a linear cost for the exchange areas ($\mathbf{d}$), and the third term includes a linear cost function associated with the consumption of hot and cold utilities, $\mathbf{z}_p$, for all operating points p.

An important assumption to be noticed in model A1-M is that the outlet streams of each heat exchanger are isothermally mixed at every stage. Therefore, the heat balances associated to the mixers are not considered. With this assumption, the only non-linear constraints are those associated with the design function $\mathbf{g}$ (i.e., the area of heat and utility exchangers), which are defined in eqs. (2) to (4).

$$\frac{q^p_{i,j,k}}{(a_{i,j,k})^{1/\beta}} - \frac{2}{3}\mathrm{U}_{i,j}\sqrt{\Delta t_{\mathrm{h}}{}^p_{i,j,k}\Delta t_{\mathrm{c}}{}^p_{i,j,k}} - \frac{1}{6}\mathrm{U}_{i,j}\sqrt{\Delta t_{\mathrm{h}}{}^p_{i,j,k}} - \frac{1}{6}\mathrm{U}_{i,j}\sqrt{\Delta t_{\mathrm{c}}{}^p_{i,j,k}} \leq 0 \tag{2}$$

$$\frac{q_{\mathrm{cu}}{}^p_i}{(a_{\mathrm{cu}i})^{1/\beta}} - \frac{2}{3}\mathrm{U}_{\mathrm{cu}i}\sqrt{\Delta t_{\mathrm{cu}}{}^p_i\Delta \mathrm{t}^*_{\mathrm{cu}i}} - \frac{1}{6}\mathrm{U}_{\mathrm{cu}i}\sqrt{\Delta t_{\mathrm{cu}}{}^p_i} - \frac{1}{6}\mathrm{U}_{\mathrm{cu}i}\sqrt{\Delta \mathrm{t}^*_{\mathrm{cu}i}} \leq 0 \tag{3}$$

$$\frac{q_{\mathrm{hu}}{}^p_j}{(a_{\mathrm{hu}j})^{1/\beta}} - \frac{2}{3}\mathrm{U}_{\mathrm{hu}j}\sqrt{\Delta t_{\mathrm{hu}}{}^p_j\Delta \mathrm{t}^*_{\mathrm{hu}j}} - \frac{1}{6}\mathrm{U}_{\mathrm{hu}j}\sqrt{\Delta t_{\mathrm{hu}}{}^p_j} - \frac{1}{6}\mathrm{U}_{\mathrm{hu}j}\sqrt{\Delta \mathrm{t}^*_{\mathrm{hu}j}} \leq 0, \tag{4}$$

Here, the variables a, a_{cu}, and a_{hu} are the areas of heat exchangers, cold utility exchangers, and hot utility exchangers, raised to the power of β, the variables q, q_{cu}, and q_{hu} are the heats associated to these units, and the variables Δt are used to calculate the temperature

difference between cold and hot stream. Moreover, in order to guarantee that the expressions $q/a^{\frac{1}{\beta}}$ are the only non-convex terms in these constraints, the approximation proposed by Paterson[34] is used. Hence, A1-M is a nonconvex MINLP model with convex objective function and nonconvex feasible region. For this type of problems it is well known that local optimality solvers can either obtain suboptimal solutions or, even worse, not find any feasible solution. Thus, a more robust optimization strategy is required to ensure that the global optimal solution of A1-M is found.

2.1.2 Flexibility Index

The flexibility problem proposed by Swaney and Grossmann[35] aims to determine the largest scaled hyper-rectangle that can be contained within the feasible region of a given design. In the context of the proposed methodology, a specific HEN design (denoted as $\mathbf{\Phi}^P$) is obtained at each iteration P. This design is determined by the fixed values of the existence binary variables and the design variables included in the solution of the multi-period formulation at iteration P ($\mathbf{\Phi}^P = \langle \mathbf{y}^{(\mathrm{fx})}, \mathbf{d}^{(\mathrm{fx})} \rangle^P$). Using this design, subsets of relevant equality constraints I' ($\mathbf{H}(\mathbf{x}_p, \mathbf{z}_p, \mathbf{\Phi}^P, \boldsymbol{\theta}_p) = 0$) and relevant inequality constraints J' ($\mathbf{F}(\mathbf{x}_p, \mathbf{z}_p, \mathbf{\Phi}^P, \boldsymbol{\theta}_p) \leq 0$) are selected from eqs. (1b) and (1c), respectively. These equalities and inequalities, given by the systems of equations (5) and (6), represent the operation of the design $\mathbf{\Phi}^P$. Here, notice

that the fixed decision variables of $\mathbf{\Phi}^P$ are denoted by the superscript '(fx)'.

$$\mathbf{H}(\mathbf{x}_p, \mathbf{z}_p, \mathbf{\Phi}^P, \boldsymbol{\theta}_p) = \left\{ \begin{array}{l} \sum_{\forall j \in J} q^p_{i,j,k} - \mathrm{F_h}^p_i (t_{\mathrm{h}}{}^p_{i,k} - t_{\mathrm{h}}{}^p_{i,k+1}) \\ \sum_{\forall i \in I} q^p_{i,j,k} - \mathrm{F_c}{}^p_j (t_{\mathrm{c}}{}^p_{j,k} - t_{\mathrm{c}}{}^p_{j,k+1}) \\ q_{\mathrm{cu}}{}^p_i - \mathrm{F_h}{}^p_i (t_{\mathrm{h}}{}^p_{i,\mathrm{N_T}+1} - \mathrm{T}_{\mathrm{hout}i}) \\ q_{\mathrm{hu}}{}^p_j - \mathrm{F_c}{}^p_j (\mathrm{T}_{\mathrm{cout}j} - t_{\mathrm{c}}{}^p_{i,1}) \\ \mathrm{T_{hin}}{}^p_i - t_{\mathrm{h}}{}^p_{i,1} \\ \mathrm{T_{cin}}{}^p_j - t_{\mathrm{c}}{}^p_{j,\mathrm{N_T}+1} \\ q^p_{i,j,k} \quad (\text{if } y^{(\mathrm{fx})}_{i,j,k} = 0) \\ q_{\mathrm{cu}}{}^p_i \quad (\text{if } y_{\mathrm{cu}}{}^{(\mathrm{fx})}_i = 0) \\ q_{\mathrm{hu}}{}^p_j \quad (\text{if } y_{\mathrm{hu}}{}^{(\mathrm{fx})}_j = 0) \\ \forall i \in I, \quad j \in J, \quad k \in K \end{array} \right\} = 0 \tag{5}$$

$$\mathbf{F}(\mathbf{x}_p, \mathbf{z}_p, \mathbf{\Phi}^P, \boldsymbol{\theta}_p) = \left\{ \begin{array}{l} t_{\mathrm{h}}{}^p_{i,k+1} - t_{\mathrm{h}}{}^p_{i,k} \\ t_{\mathrm{c}}{}^p_{j,k+1} - t_{\mathrm{c}}{}^p_{j,k} \\ \mathrm{T}_{\mathrm{hout}i} - t_{\mathrm{h}}{}^p_{i,\mathrm{N_T}+1} \\ t_{\mathrm{c}}{}^p_{j,1} - \mathrm{T}_{\mathrm{cout}j} \\ \Delta\mathrm{T}_{\min} + t_{\mathrm{c}}{}^p_{j,k} - t_{\mathrm{h}}{}^p_{i,k} \quad (\text{if } y^{(\mathrm{fx})}_{i,j,k} = 1) \\ \Delta\mathrm{T}_{\min} + t_{\mathrm{c}}{}^p_{j,k+1} - t_{\mathrm{h}}{}^p_{i,k+1} \quad (\text{if } y^{(\mathrm{fx})}_{i,j,k} = 1) \\ \Delta\mathrm{T}_{\min} + \mathrm{T_{cuout}} - t_{\mathrm{h}}{}^p_{i,\mathrm{N_T}+1} \quad (\text{if } y_{\mathrm{cu}}{}^{(\mathrm{fx})}_i = 1) \\ \Delta\mathrm{T}_{\min} + t_{\mathrm{c}}{}^p_{j,1} - \mathrm{T_{huout}} \quad (\text{if } y_{\mathrm{hu}}{}^{(\mathrm{fx})}_j = 1) \\ \forall i \in I, \quad j \in J, \quad k \in K \end{array} \right\} \leq 0 \tag{6}$$

Grossmann and Floudas[36] reformulate the flexibility problem as a single-level MINLP optimization problem (FI-M), where the inner minimization problem is replaced by the Karush-Kuhn-Tucker optimality conditions (KKT). With this approach both flow and temperature variations of the inlet streams can be simultaneously considered. A given design is called

flexible if its flexibility index (FI) is equal to or greater than one, i.e. the design is able to operate within the range of expected variation. The formulation FI-M is presented in eq. (7),

Problem FI-M:

$$FI^P = \min_{\mathbf{x}_\mathrm{F}, \mathbf{y}_\mathrm{F}} \quad \delta \tag{7a}$$

$$\text{s.t.} \quad F_{j'}(\mathbf{x}_{P+1}, \mathbf{z}_{P+1}, \mathbf{\Phi}^P, \boldsymbol{\theta}^*_{P+1}) + s_{j'} = 0, \quad \forall j' \in J' \tag{7b}$$

$$H_{i'}(\mathbf{x}_{P+1}, \mathbf{z}_{P+1}, \mathbf{\Phi}^P, \boldsymbol{\theta}^*_{P+1}) = 0, \quad \forall i' \in I' \tag{7c}$$

$$\sum_{j' \in J'} \lambda_{j'} = 1 \tag{7d}$$

$$\sum_{j' \in J'} \lambda_{j'} \frac{\partial F_{j'}}{\partial \mathbf{z}_{P+1}} + \sum_{i' \in I'} \mu_{i'} \frac{\partial H_{i'}}{\partial \mathbf{z}_{P+1}} = 0 \tag{7e}$$

$$\sum_{j' \in J'} \lambda_{j'} \frac{\partial F_{j'}}{\partial \mathbf{x}_{P+1}} + \sum_{i' \in I'} \mu_{i'} \frac{\partial H_{i'}}{\partial \mathbf{x}_{P+1}} = 0 \tag{7f}$$

$$\lambda_{j'} - y^\mathrm{F}_{j'} \leq 0, \quad \forall j' \in J' \tag{7g}$$

$$s_{j'} - \mathrm{M_F}(1 - y^\mathrm{F}_{j'}) \leq 0, \quad \forall j' \in J' \tag{7h}$$

$$\sum_{j' \in J'} y^\mathrm{F}_{j'} \leq n_z + 1 \tag{7i}$$

$$\boldsymbol{\theta}_1 - \delta \Delta \boldsymbol{\theta}^- \leq \boldsymbol{\theta}^*_{P+1} \leq \boldsymbol{\theta}_1 + \delta \Delta \boldsymbol{\theta}^+ \tag{7j}$$

$$\delta \geq 0, y^\mathrm{F}_{j'} = \{0, 1\}, \lambda_{j'} \geq 0, s_{j'} \geq 0, \forall j' \in J' \tag{7k}$$

$$\mathbf{x}_\mathrm{F} = \langle \mathbf{x}_{P+1},\, \mathbf{z}_{P+1},\, \mu_{i'},\, \lambda_{j'},\, \boldsymbol{\theta}^*_{P+1},\, \mathbf{s}_{j'},\, \delta \rangle, \quad \mathbf{y}_\mathrm{F} = \langle y^\mathrm{F}_{j'} \rangle$$

where FI^P is the flexibility index at iteration P, $s_{j'}$ and $\lambda_{j'}$ are the slack variables and the Lagrange multipliers, respectively, of the inequalities j', $\mu_{i'}$ are the Lagrange multipliers associated to the equality constraints i', the binary variables $y^\mathrm{F}_{j'}$ are used to represent if the inequality constraints j' are active (when $y^\mathrm{F}_{j'} = 1$), $\mathrm{M_F}$ is an upper bound for the slack variables $s_{j'}$, and n_z is the number of control variables selected. Notice that the sets $\mathbf{x}_\mathrm{F}$ and $\mathbf{y}_\mathrm{F}$ aggregate all the continuous and binaries variables, respectively, used for the optimization. The meaning of $\boldsymbol{\theta}^*_p$ is equivalent to $\boldsymbol{\theta}_p$. However, $\boldsymbol{\theta}^*_p$ is a continuous variable in the problem

FI-M, whereas $\boldsymbol{\theta}_p$ is used as a parameter in the problem of synthesis. In particular, the variables $\boldsymbol{\theta}_p^*$ are obtained by solving the problem FI-M and used to calculate the parameters $\boldsymbol{\theta}_p$. Also, it is worth mentioning that all potential control manipulations ($\mathbf{z}_{P+1}$) are considered at the flexibility analysis stage to achieve feasible operation.

Substituting eqs. (5) and (6) in the formulation presented in eq. (7) it is possible to solve the model FI-M. At eq. (7j), the problem is evaluated with respect to the nominal operating point ($\boldsymbol{\theta}_1$) since the aim of FI-M is to obtain the maximum possible deviation from this point allowed by the design. In this sense, δ represents the fraction of the maximum expected disturbances ($\Delta\boldsymbol{\theta}^+$, $\Delta\boldsymbol{\theta}^-$) supported by the design.

Finally, based on the solution of FI-M a new critical point $\boldsymbol{\theta}_{\mathrm{P+1}}$ is identified at each iteration P. To calculate this new critical point a small increase is added to $\boldsymbol{\theta}^*_{\mathrm{P+1}}$ in the direction $\boldsymbol{\Gamma}$ that this point deviates from the nominal point (i.e., $\boldsymbol{\theta}_{\mathrm{P+1}} = \boldsymbol{\theta}^*_{\mathrm{P+1}} + \boldsymbol{\Gamma}\epsilon$). It is important to note that a single critical point is obtained at each iteration P by solving the model FI-M.

2.2 Optimization Strategy

The optimization strategy proposed by Björk and Westerlund [13] is applied, where the non-convex terms of A1-M are replaced by convex approximations that guarantee the optimality of the solution. This strategy relies on convexifying the signomial terms presented in eqs. (2) to (4) to obtain a convex formulation. Thus, the new problem is a relaxation of the feasible region (i.e., an approximation) of the original problem. The strategy is based on solving a sequence of original and approximate subproblems in order to find the optimal solution. The optimal objective values of these subproblems become upper and lower bounds of the model A1-M, which are referred as $A1^{P,L}_{\mathrm{ub}}$ and $A1^{P,L}_{\mathrm{lb}}$, respectively. While the index P still denotes the iterations of the flexible synthesis procedure, the index L is introduced to indicate the iterations required to solve each model A1-M. At each iteration L an approximate model is solved and, based on its solution, a new grid point is added. Thus, the formulation becomes

more accurate and a tighter lower bound is obtained. This strategy allows the difference between the lower bound ($A1_{\text{lb}}^{P,L}$) and best upper bound (denoted as $A1_{\text{ub}}^{P,*}$) at iteration L to be used as the convergence criterion.

In order to solve each approximate model, the outer approximation technique proposed by Viswanathan and Grossmann[33] is used. This strategy is based on solving a series of mixed-integer linear programming (MILP) and non-linear programming (NLP) subproblems to obtain the lower and upper bounds of the relaxed problem (referred as $A2_{\text{lb}}^{P,L}$ and $A2_{\text{ub}}^{P,L}$, respectively). In the following sections the required convexification technique and outer approximation procedure are briefly revisited.

2.2.1 Covexification of signomial terms

The main idea here is to convexify the signomial terms $q/(a^{\frac{1}{\beta}})$ present in the model by considering the transformation $q = \exp(Q)$. Hence, the non-convex terms are replaced based on the following expression:

$$\frac{q}{a^{1/\beta}} = \frac{\exp(Q)}{a^{1/\beta}} \tag{8}$$

which is convex on $\mathbb{R}^+$. The inverse transformation function:

$$Q = \ln(q) \tag{9}$$

is nonconvex and, therefore, a piece-wise linear representation of eq. (9) is used to convexify the model. This piece-wise linear representation will underestimate $\ln(q)$ and provide an approximate value for Q. Thus, the solution of the convexified problem will be an approximation of the solution to the original problem. This approximation will be exact if the value of Q is equivalent to a gridpoint limit (i.e., the bound of some interval for the piece-wise approximation). The general structure of the approximate convex model is shown in eq. (10).

Problem A2-M:

$$A2^{P,L} = \min_{\mathbf{x}_C, \mathbf{y}_C} \ \mathbf{c_f y} + \mathbf{c_d d} + \sum_{p=1}^{P} C(\mathbf{z}_p) \tag{10a}$$

$$\text{s.t.} \quad \mathbf{A y} + \mathbf{B y}'_p + \mathbf{h}(\mathbf{x}_p, \mathbf{z}_p, \mathbf{d}, \boldsymbol{\theta}_p) = 0, \tag{10b}$$

$$\mathbf{C y} + \mathbf{D y}'_p + \mathbf{f}(\mathbf{x}_p, \mathbf{z}_p, \mathbf{d}, \boldsymbol{\theta}_p) \leq 0, \tag{10c}$$

$$\mathbf{g}^{\mathrm{c}}(\mathbf{x}_p, \mathbf{dz}_p, \mathbf{d}, \boldsymbol{\theta}_p) \leq 0, \tag{10d}$$

$$\mathbf{D}_{\mathrm{L}}(\mathbf{z}_p, \mathbf{dz}_p, \mathbf{w}_p) = 0, \tag{10e}$$

$$\mathbf{x}_p^{LO} \leq \mathbf{x}_p \leq \mathbf{x}_p^{UP}, \quad \mathbf{x}_p \in \mathbb{R}^n \tag{10f}$$

$$\mathbf{z}_p^{LO} \leq \mathbf{z}_p \leq \mathbf{z}_p^{UP}, \quad \mathbf{z}_p \in \mathbb{R}^q, \tag{10g}$$

$$\mathbf{dz}_p^{LO} \leq \mathbf{dz}_p \leq \mathbf{dz}_p^{UP}, \quad \mathbf{dz}_p \in \mathbb{R}^{q \times L}, \tag{10h}$$

$$\mathbf{d}^{LO} \leq \mathbf{d} \leq \mathbf{d}^{UP}, \quad \mathbf{d} \in \mathbb{R}^q \tag{10i}$$

$$\mathbf{y} \in \{0,1\}^q, \quad \mathbf{y}'_p \in \{0,1\}^q, \quad \mathbf{w}_p \in \{0,1\}^{q \times L} \tag{10j}$$

$$\forall p = 1, \ldots, P \tag{10k}$$

$$\mathbf{x}_{\mathrm{C}} = \langle \mathbf{x}_p, \mathbf{dx}_p, \mathbf{z}_p, \mathbf{dz}_p, \mathbf{d} \rangle, \quad \mathbf{y}_{\mathrm{C}} = \langle \mathbf{y}, \mathbf{y}'_p, \mathbf{w}_p \rangle$$

In eq. (10), $A2^{P,L}$ is the value of the economic objective function for iterations P and L, considering P operating points in the flexible synthesis problem and L gridpoints for the piece-wise approximation. This value represents the lower bound of the original model and, therefore, is used to set $A1_{\mathrm{lb}}^{P,L}$. The function $\mathbf{D}_{\mathrm{L}}(\mathbf{z}_p, \mathbf{dz}_p, \mathbf{w}_p)$ represents the formulation of the piecewise relaxation, where the matrix $\mathbf{dz}_p \in \mathbb{R}^{q \times L}$ includes the new continuous variables (Q) and $\mathbf{w}_p \in \{0,1\}^{q \times L}$ are the binary variables associated to grid interval selection. These new variables are defined for each possible exchanged heat and each grid interval $l = 1, \ldots, L$. In eq. (10d), notice that the nonconvex constraints are convexified by replacing the functions $\mathbf{g}$ with their convex counterparts $\mathbf{g}^{\mathrm{c}}$. The variable sets $\mathbf{x}_{\mathrm{C}}$ and $\mathbf{y}_{\mathrm{C}}$ aggregate all the optimization continuous and binaries variables, respectively. At each iteration L, the size of the grid is increased by considering an additional gridpoint based on the previous solution of the

approximate model. Thus, the new problem becomes more accurate and the lower bound ($A1_{\text{lb}}^{P,L}$) increases. The gap between this lower bound and the best upper bound ($A1_{\text{ub}}^{P,*}$) is considered as the stopping criterion. It is important to recall that the size of problem A2-M increases when more periods (P) or more gridpoints (L) are considered. The complete set of constraints for model A2-M is presented in the Supporting Information File. To solve each model A2-M an outer-approximation procedure is used, and a brief description of this strategy is presented in the following section.

2.2.2 Outer-approximation procedure

The MINLP optimization strategy based on the Augmented-Penalty-function / Outer- Approximation / Equality-Relaxation (AP/OA/ER) algorithm proposed by Viswanathan and Grossmann[33] is used to solve each subproblem A2-M. The iteration number of the outer-approximation procedure is denoted as R. The algorithm starts ($R = 0$) by solving the relaxation of the MINLP model given by eq. (10) and, if a non-integer solution is found, a sequence of MILP master problems and NLP subproblems are solved. The optimal objective values of the MILP and NLP problems are the lower ($A2_{\text{lb}}^{P,L,R}$) and upper ($A2_{\text{ub}}^{P,L,R}$) bounds, respectively, of the formulation A2-M for each iteration R. Considering a given multi-period iteration (P) and an approximation (L), the NLP subproblem shown in eq. (11) is derived from formulation A2-M by fixing the set of binary variables $(\mathbf{y_C}^R = \langle \mathbf{y}^R, \mathbf{y'}_p^R, \mathbf{w}_p^R \rangle)^{P,L}$ obtained at iteration R.

Problem A2-NLP:

$$A2_{\text{ub}}^{P,L,R} = \min_{\mathbf{x}_\text{C}} \ \mathbf{c_f}\mathbf{y}^R + \mathbf{c_d}\mathbf{d} + \sum_{p=1}^{\text{N}_\text{P}} C(\mathbf{z}_p) \tag{11a}$$

$$\text{s.t.} \quad \mathbf{A}\mathbf{y}^R + \mathbf{B}\mathbf{y}_p'^R + \mathbf{h}(\mathbf{x}_p, \mathbf{z}_p, \mathbf{d}, \boldsymbol{\theta}_p) = 0, \tag{11b}$$

$$\mathbf{C}\mathbf{y}^R + \mathbf{D}\mathbf{y}_p'^R + \mathbf{f}(\mathbf{x}_p, \mathbf{z}_p, \mathbf{d}, \boldsymbol{\theta}_p) \leq 0, \tag{11c}$$

$$\mathbf{g}^\text{c}(\mathbf{x}_p, \mathbf{dz}_p, \mathbf{d}, \boldsymbol{\theta}_p) \leq 0, \tag{11d}$$

$$\mathbf{D}_\text{L}(\mathbf{z}_p, \mathbf{dz}_p, \mathbf{w}_p^R) = 0, \tag{11e}$$

$$\mathbf{x}_p^{LO} \leq \mathbf{x}_p \leq \mathbf{x}_p^{UP}, \quad \mathbf{x}_p \in \mathbb{R}^n \tag{11f}$$

$$\mathbf{z}_p^{LO} \leq \mathbf{z}_p \leq \mathbf{z}_p^{UP}, \quad \mathbf{z}_p \in \mathbb{R}^q, \tag{11g}$$

$$\mathbf{dz}_p^{LO} \leq \mathbf{dz}_p \leq \mathbf{dz}_p^{UP}, \quad \mathbf{dz}_p \in \mathbb{R}^{q\times L}, \tag{11h}$$

$$\mathbf{d}^{LO} \leq \mathbf{d} \leq \mathbf{d}^{UP}, \quad \mathbf{d} \in \mathbb{R}^q \tag{11i}$$

$$\forall p = 1, \ldots, P \tag{11j}$$

$$\mathbf{x}_\text{C} = \langle \mathbf{x}_p,\, \mathbf{dx}_p,\, \mathbf{z}_p,\, \mathbf{dz}_p,\, \mathbf{d} \rangle,$$

In turn, these binary decisions ($\mathbf{y}_\text{C}{}^R$) are obtained by solving the MILP master problem, which is generated from the last NLP solutions. If $\mathbf{x}_\text{C}{}^0$ is the solution of the relaxed MINLP and $\mathbf{x}_\text{C}{}^r$, with $r = 1, \ldots, R-1$, are the previously-determined NLP solutions obtained by fixing the binary decisions $\mathbf{y}_\text{C}{}^r$, then the MILP for determining the integer vector $\mathbf{y}_\text{C}{}^R$ is represented as shown in eq. (12).

Problem A2-MIP:

$$A2_{\mathrm{lb}}^{P,L,R} = \min_{\mathbf{x}_{\mathrm{C}},\mathbf{y}_{\mathrm{C}}} \ \mathbf{c_f y} + \alpha + \sum_{r=0}^{R-1} \mathbf{wk}_r \, \boldsymbol{s}_r \tag{12a}$$

$$\text{s.t.} \quad \mathbf{A y} + \mathbf{B y}'_p + \mathbf{h}(\mathbf{x}_p, \mathbf{z}_p, \mathbf{d}, \boldsymbol{\theta}_p) = 0, \tag{12b}$$

$$\mathbf{C y} + \mathbf{D y}'_p + \mathbf{f}(\mathbf{x}_p, \mathbf{z}_p, \mathbf{d}, \boldsymbol{\theta}_p) \le 0, \tag{12c}$$

$$\mathbf{g}^{\mathrm{c}}(\mathbf{x}_p^r, \mathbf{dz}_p^r, \mathbf{d}, \boldsymbol{\theta}_p) + \nabla \mathbf{g}^{\mathrm{c}}(\mathbf{x}_p^r, \mathbf{dz}_p^r, \mathbf{d}, \boldsymbol{\theta}_p)^{\mathrm{T}} \begin{bmatrix} (\mathbf{x}_p - \mathbf{x}_p^r) \\ (\mathbf{dz}_p - \mathbf{dz}_p^r) \end{bmatrix} \le \boldsymbol{s}_r, \tag{12d}$$

$$\mathbf{D}_{\mathrm{L}}(\mathbf{z}_p, \mathbf{dz}_p, \mathbf{w}_p) = 0, \tag{12e}$$

$$\mathbf{c_d d} + \sum_{p=1}^{P} C(\mathbf{z}_p) - \alpha \le 0, \tag{12f}$$

$$(2\,\mathbf{y}^r - \mathbf{1}_m)\mathbf{y} - |\mathbf{y}^r|_1 + \sum_{p=1}^{P} \Big[(2\,\mathbf{y'}_p^r - \mathbf{1}_m)\mathbf{y}'_p - |\mathbf{y'}_p^r|_1 \Big] + \sum_{p=1}^{P} \phi\Big([2\,\mathbf{w}_p^r - \mathbf{1}_{q\times L}] \otimes \mathbf{w}_p - \mathbf{w}_p^r \Big) + 1 \le 0 \quad (r \ne 0), \tag{12g}$$

$$\mathbf{x}_p^{LO} \le \mathbf{x}_p \le \mathbf{x}_p^{UP}, \quad \mathbf{x}_p \in \mathbb{R}^n \tag{12h}$$

$$\mathbf{z}_p^{LO} \le \mathbf{z}_p \le \mathbf{z}_p^{UP}, \quad \mathbf{z}_p \in \mathbb{R}^q, \tag{12i}$$

$$\mathbf{dz}_p^{LO} \le \mathbf{dz}_p \le \mathbf{dz}_p^{UP}, \quad \mathbf{dz}_p \in \mathbb{R}^{q\times L}, \tag{12j}$$

$$\mathbf{d}^{LO} \le \mathbf{d} \le \mathbf{d}^{UP}, \quad \mathbf{d} \in \mathbb{R}^q \tag{12k}$$

$$\boldsymbol{s}_r \ge 0, \quad \boldsymbol{s}_r \in \mathbb{R}^m \tag{12l}$$

$$\mathbf{y} \in \{0,1\}^q, \quad \mathbf{y}'_p \in \{0,1\}^q, \quad \mathbf{w}_p \in \{0,1\}^{q\times L} \tag{12m}$$

$$\forall p = 1, \ldots, P, \quad \forall r = 0, \ldots, R-1 \tag{12n}$$

$$\mathbf{x}_{\mathrm{C}} = \langle \mathbf{x}_p,\, \mathbf{dx}_p,\, \mathbf{z}_p,\, \mathbf{dz}_p,\, \mathbf{d} \rangle, \quad \mathbf{y}_{\mathrm{C}} = \langle \mathbf{y},\, \mathbf{y}'_p,\, \mathbf{w}_p \rangle$$

In eq. (12), the parameters $\mathbf{wk}_r = [wk_{r,\kappa}]$ are the weights of the slack variables $\boldsymbol{s}_r$. These parameters must satisfy the condition $wk_{r,\kappa} > |\mu_{r,\kappa}|$, where $\mu_{r,\kappa}$ are the KKT multipliers associated with the κ-th inequality constraints g_κ and obtained from the NLP problem solved

at iteration r. Through consecutive iterations R, new linearizations (eq. 12d) and integer cuts (eq. 12g) are added to each A2-MIP formulation and, therefore, the lower bound of $A2^{P,L}$ increases. These integer cuts are introduced to eliminate the previously-determined integer vectors $(\mathbf{y_C}^1)^{L,P}$, $(\mathbf{y_C}^2)^{L,P}$, ... , $(\mathbf{y_C}^{R-1})^{L,P}$. In eq. (12g), $\mathbf{1}_m$ is the vector of ones of size m, $\mathbf{1}_{q\times L}$ is the matrix of ones of size $q \times L$, $\otimes$ is the Hadamard product (entrywise product), $|\cdot|_1$ is the 1-norm of vectors, and the function $\phi(\cdot)$ is the element-by-element summation for matrices (for binary vectors, notice that $|\cdot|_1$ is also the respective element-by-element summation). An important observation is that the convexification technique applied to obtain A2-M guarantees that the solutions of the formulations A2-MIP are valid lower bounds for the objective function of the relaxed problem. Since integer cuts are incorporated at each iteration, the algorithm stops when the lower bound is greater than the best upper bound (denoted as $A2^{P,L,*}_{\text{ub}}$). When such crossover occurs, the best upper bound obtained by the OA strategy is the final solution of the current A2-M formulation. Moreover, this best upper bound is actually the lower bound of the original model (A1-M) because the model A2-NLP is equal to the problem A2-M with fixed binary decisions and, therefore, $A1^{P,L}_{lb}$=$A2^{P,L,*}_{\text{ub}}$. Recall that a sequence of MILP and NLP formulations is solved for each period (P) and relaxation (L) to obtain this solution.

2.3 Control Structure Design

Once an optimal and flexible HEN is obtained, the control structure design (CSD) problem is addressed. Here, the methodologies of Braccia et al.[37] and Zumoffen[38] are considered as a starting point. These methodologies are based on the combination of two steady-state indexes: the sum of squared deviations (SSD), which handles controlled variables (CVs) and manipulated variables (MVs) selection, and the net load evaluation (NLE), which defines the structure of the controller. The approach of Zumoffen[38] is formulated as a bilevel mixed-integer nonlinear programming (BMINLP) problem, where discrete decisions are included in both the upper and lower-level optimization problems. This problem has been reformulated

using mixed-integer quadratic programming (MIQP) by Braccia et al.[37]. The new model featured both optimality and improved computational performance due to the use of state-of-the-art solvers.

In the proposed work, the control structure of the HEN is designed by only minimizing the SSD index and selecting the MVs, since all the process output variables (output temperatures) need to be controlled. In this context, the approach by Braccia et al.[37] is simplified by only considering the SSD index evaluation, required to perform the control structure selection, based on the deviations of the MVs. A transfer function matrix (TFM) representation (Laplace domain) of the stable or already stabilized HEN, $\mathbf{y}(s) = \mathbf{G}(s)\mathbf{u}(s) + \mathbf{D}(s)\mathbf{d}^*(s)$, is considered, where $\mathbf{y}(s)$ are the potential output measurements (outlet temperatures), $\mathbf{u}(s)$ are the available manipulated variables (bypass flow fractions and flowrates of utility exchangers), and $\mathbf{d}^*(s)$ are the disturbance variables (inlet temperatures and flowrates) with size $(1 \times M')$, $(N' \times 1)$ and $(D' \times 1)$, respectively. This system can be partitioned as:

$$\mathbf{y}_{\mathrm{s}}(s) = \begin{bmatrix} \mathbf{G}_{\mathrm{s}}(s) & \mathbf{G}^*_{\mathrm{s}}(s) \end{bmatrix} \begin{bmatrix} \mathbf{u}_{\mathrm{s}}(s) \\ \mathbf{u}_{\mathrm{r}}(s) \end{bmatrix} + \mathbf{D}_{\mathrm{s}}(s)\mathbf{d}^*(s) \tag{13}$$

where $\mathbf{y}_{\mathrm{s}}(s)$ are the selected controlled variables (CVs), $\mathbf{u}_{\mathrm{s}}(s)$ are the selected manipulated variables (MVs) to control the subprocess $\mathbf{G}_{\mathrm{s}}(s)$, and $\mathbf{u}_{\mathrm{r}}(s) = 0$ are not used. To perform this partition, the single level mixed-integer quadratic problem considered in this work is shown in eq. (14).

Problem SSD-M:

$$SSD^p = \min_{\mathbf{u},\mathbf{y},\mathbf{z}} \quad \sum_{\sigma=1}^{M'} \sum_{\ell=1}^{N'} \left(u^{\mathrm{c}p}_{\ell,\sigma}\right)^2 + \sum_{\omega=1}^{D'} \sum_{\ell=1}^{N'} \left(u^{\mathrm{d}p}_{\ell,\omega}\right)^2 \tag{14a}$$

$$\text{s.t.} \quad \sum_{\ell=1}^{N'} g^p_{\nu,\ell}\, u^{\mathrm{c}p}_{\ell,\sigma} - \phi_{\nu,\sigma} = 0, \tag{14b}$$

$$\sum_{\ell=1}^{N'} g^p_{\nu,\ell}\, u^{\mathrm{d}p}_{\ell,\omega} + d_{\nu,\omega} = 0 \tag{14c}$$

$$-\,\mathrm{M_S} z^{\mathrm{I}p}_{\ell} \le u^{\mathrm{c}p}_{\ell,\sigma} \le \mathrm{M_S} z^{\mathrm{I}p}_{\ell}, \tag{14d}$$

$$-\,\mathrm{M_S} z^{\mathrm{I}p}_{\ell} \le u^{\mathrm{d}p}_{\ell,\omega} \le \mathrm{M_S} z^{\mathrm{I}p}_{\ell}, \tag{14e}$$

$$\sum_{\ell=1}^{N'} z^{\mathrm{I}p}_{\ell} = \mathrm{N_H} + \mathrm{N_C} \tag{14f}$$

$$-\,\mathrm{M_S}(1 - z^{\mathrm{nd}p}_{\sigma,\ell}) \le y^{\mathrm{r}p}_{\sigma,\ell} - g^p_{\sigma,\ell}\, u^{\mathrm{c}p}_{\ell,\sigma} \le \mathrm{M_S}(1 - z^{\mathrm{nd}p}_{\sigma,\ell}), \tag{14g}$$

$$\sum_{\nu=1}^{M'} z^{\mathrm{nd}p}_{\nu,\ell} = z^{\mathrm{I}p}_{\ell}, \quad \sum_{\ell=1}^{N'} z^{\mathrm{nd}p}_{\nu,\ell} = 1, \tag{14h}$$

$$\delta_1 z^{\mathrm{nd}p}_{\sigma,\ell} \le y^{\mathrm{r}p}_{\sigma,\ell} \le \delta_2 z^{\mathrm{nd}p}_{\sigma,\ell}, \tag{14i}$$

$$\forall \sigma = 1, \ldots, M', \quad \forall \nu = 1, \ldots, M', \tag{14j}$$

$$\forall \omega = 1, \ldots, D', \quad \forall \ell = 1, \ldots, N' \tag{14k}$$

The optimal solution SSD^p is the sum of squared deviations index for the optimal HEN working at the operating point p (where the index p represents either the nominal point or the critical points obtained at the synthesis stage). Moreover, $\mathbf{G}^p = [g^p_{\nu,\ell}]$ and $\mathbf{D}^p = [d^p_{\nu,\omega}]$ are constant matrices of size $(M' \times N')$ and $(M' \times D')$, which represent the normalized HEN model for each operating point p, where N', M', and D' are the number of total inputs (the bypass of heat exchangers and the flowrate ofutility exchangers), outputs (outlet temperatures), and perturbations (inlet temperatures and flowrates), respectively. The parameter $\phi_{\nu,\sigma}$ is the (ν, σ)-th entry of the $(M' \times M')$ identity matrix. Since a normalized system is used, this parameter represents the change of the output variables set-point.

For simplicity, in the next paragraphs the superscript representing the operating point (p) is dropped (e.g., ${u^{c}}^{p}_{\ell,\sigma} = {u^{c}}_{\ell,\sigma}$), since the discussion that follows is valid for every operating point. If set point changes and disturbances are considered separately, the big-M formulation given in eqs. (14b) to (14f) is equivalent to the following systems of equations for each set point change σ and for each disturbance change ω:

$$\text{Set point changes:} \quad \begin{cases} \mathbf{G}\mathbf{u}^{\mathrm{c}}_{\sigma} - \mathbf{v}_{\sigma} = 0 & \forall\, \sigma \in \text{CVs} \\ \text{non selected MVs in } \mathbf{u}^{\mathrm{c}}_{\sigma} \text{ fixed to zero} \end{cases}$$

$$\text{Disturbance changes:} \quad \begin{cases} \mathbf{G}\mathbf{u}^{\mathrm{d}}_{\omega} + \mathbf{D}\mathbf{v}_{\omega} = 0 & \forall\, \omega = 1, \ldots, D' \\ \text{non selected MVs in } \mathbf{u}^{\mathrm{d}}_{\omega} \text{ fixed to zero} \end{cases} \tag{15}$$

In eq. (15), $\mathbf{v}_{\sigma}$ and $\mathbf{v}_{\omega}$ are unitary vectors of size $(M' \times 1)$ and $(D' \times 1)$, respectively. The equations (14b) to (14f) are defined to obtain the deviations of the input variables $\mathbf{u}^{\mathrm{c}}_{\sigma} = [{u^{\mathrm{c}}}_{\ell,\sigma}]$ and $\mathbf{u}^{\mathrm{d}}_{\omega} = [{u^{\mathrm{d}}}_{\ell,\omega}]$. These vectors are associated, respectively, to the individual set point change of each controlled output σ, and to the individual change of each disturbance ω. The entries of $\mathbf{u}^{\mathrm{c}}_{\sigma}$ and $\mathbf{u}^{\mathrm{d}}_{\omega}$ which are not selected as MVs are driven to zero. Indeed, eqs. (14d) and (14e) constraint the MVs using the binary variables $\mathbf{z}^{\mathrm{I}} = [z^{\mathrm{I}}_{\ell}]$. The entries of the vector $\mathbf{z}^{\mathrm{I}}$ with unitary value indicate the MVs selected for the control structure. This approach allows selecting specific parts of $\mathbf{G}$ to obtain the subprocess $\mathbf{G}_{\mathrm{s}}$ using big-M constraints while avoiding the non-linearities introduced in the original formulation [38].

As a result, the SSD index in eq. (14a) quantifies the deviations of the manipulated variables ($\mathbf{u}$) required when set point changes and disturbances take place separately. The SSD minimization properties were extensively analyzed in Zumoffen [38] and Zumoffen and Basualdo [39], where it was shown that this minimization tends to maximize the minimum singular value of the subprocess $\mathbf{G}_{\mathrm{s}}$, i.e., the selected subprocess is easy to control. The eqs. (14f) guarantee that the number of CVs (all hot and cold output variables) and MVs are the same (square control structure)

The input-output pairing problem, eqs. (14g) to (14i), is addressed here based on the relative gain array (RGA) approach. Since a direct computation of the RGA will introduce strong non-linearities, the reformulation presented in Braccia et al.[37] is used in this work. Hence, the RGA matrix can be computed as $\Lambda = \mathbf{G} \otimes \mathbf{u}^{c}$ where $\mathbf{G}$ is a fixed real matrix and $\otimes$ the Hadamard product (element-by-element product). A new array of binary variables $\mathbf{z}^{nd} = [z^{nd}_{\sigma,\ell}]$, which represents the selected decentralized control structure, is introduced. The unitary entries in $\mathbf{z}^{nd}$ correspond to proper and feasible gains in Λ. The RGA evaluation is performed in eq. (14g) using big-M constraints associated to the corresponding decentralized control structure defined by $\mathbf{z}^{nd}$. The new continuous variable matrix $\mathbf{y}^{r} = [y^{r}{}_{\sigma,\ell}]$ holds the non-zero entries of the RGA matrix. Moreover, these entries are constrained by eqs. (14i) guaranteeing a feasible and useful input-output pairing according to the scalar parameters δ_1 and δ_2 fixed by the user. Finally, eqs. (14h) ensure that the control structure defined by $\mathbf{z}^{nd}$ has a single unitary entry at each row and column, pairing the CVs with the selection of MVs handled by $\mathbf{z}^{I}$. Recall that the problem SSD-M defined in eq. (14) is solved for both the nominal and each critical plant model ($\mathbf{G}^{p}$ and $\mathbf{D}^{p}$) after the synthesis stage.

2.4 Algorithm

A detailed step-by-step description of the proposed procedure (1) is given in the following paragraphs:

- **Step A: Multi-period Synthesis Model**

  Step A-1: Set $P = 1$ to consider nominal operating conditions for inlet flow rates and temperatures.

  Step A-2: The multi-period simultaneous synthesis formulation is solved using an optimization strategy to guarantee solution optimality. A sequence of approximate models (A2-M) are solved and original formulations (A1-M) are evaluated to obtain a lower bound ($A1^{P,L}_{lb}$) and upper bound ($A1^{P,L}_{ub}$) of the original problem.

- **Step B: Optimization based on convexification strategy**

Step B-1: Set $L = 1$, define grids for the heat exchange variables ($q^p_{i,j,k}$, qcu^p_i, qhu^p_j), and set $A1^{P,*}_{\text{ub}} = \infty$.

Step B-2: Outer-Approximation method

The outer approximation method is used to solve A2-M. The solution of this model is a lower bound ($A1^{P,L}_{\text{lb}}$) of the global optimal solution.

Step B-2.1: Solve the relaxed MINLP problem (relaxed A2-M) to determine a KKT point ($\mathbf{x}_C{}^0$, $\mathbf{y}_C{}^0$). If $\mathbf{y}_C{}^0$ is integral then the optimal solution is found, go to step B-3. Otherwise, set $R = 1$, $A2^{P,L,*}_{\text{ub}} = \infty$, and continue at step B-2.2.

Step B-2.2: Solve the MIP master problem (A2-MIP) to find the integer vector $\mathbf{y}_C{}^R$ with objective function z^R_{lb}. The solution is a lower bound of the relaxed problem, set $A2^{P,L,R}_{\text{lb}} = z^R_{\text{lb}}$.

Step B-2.3: Solve the NLP subproblem (A2-NLP) with the binary vector $\mathbf{y}_C{}^R$ fixed to determine the KKT point ($\mathbf{x}_C{}^R$) with objective function z^R_{ub}. If the NLP is infeasible set FLAG = 0. If the NLP is feasible then the solution is an upper bound of the relaxed problem, set $A2^{P,L,R}_{\text{ub}} = z^R_{\text{ub}}$, FLAG = 1.

Step B-2.4: (a) if FLAG = 1, determine if $A2^{P,L,R}_{\text{lb}} \geq A2^{P,L,*}_{\text{ub}}$ (i.e., the current lower bound is higher than the best upper bound). If satisfied, the optimal solution of formulation A2-M is the best upper bound ($A2^{P,L,*}_{\text{ub}}$), stop and go to step B-3. Otherwise, set the best upper bound $A2^{P,L,*}_{\text{ub}} = \min[A2^{P,L,R}_{\text{ub}}, A2^{P,L,*}_{\text{ub}}]$, add the corresponding linearization (eq. 12d) to improve the approximation of the nonlinear functions, add the integer cut (eq. 12g) to eliminate the binary solution ($\mathbf{y}_C{}^R$) just found, set $R = R + 1$, and return to Step B-2.2. (b) If FLAG = 0, set $R = R + 1$ and return to Step B-2.2 after adding the corresponding integer cut (eq. 12g).

Note: The best upper bound $A2^{P,L,*}_{\text{ub}}$ is a lower bound of the original problem, since the formulation A2-M is an approximation of A1-M. Therefore $A1^{P,L}_{\text{lb}} = A2^{P,L,*}_{\text{ub}}$.

Step B-3: Fix the heat exchange variables and evaluate the formulation A1-M. The solution of this model is an upper bound ($A1_{\text{ub}}^{P,L}$) of the global optimal solution.

Step B-4: If $A1_{\text{lb}}^{P,L}$ is close enough to $A1_{\text{ub}}^{P,*}$ ($|1 - A1_{\text{lb}}^{P,L}/A1_{\text{ub}}^{P,*}| \leq \varepsilon$), then set $A1^P = A1_{\text{ub}}^{P,*}$, terminate and go to step C. The optimal heat exchanger network is found with a total annual cost (TAC) equal to $A1^P$. Otherwise, set the best upper bound $A1_{\text{ub}}^{P,*} = \min[A1_{\text{ub}}^{P,*}, A1_{\text{ub}}^{P,L}]$, set $L = L + 1$, and return to step B-2 after adding the grid points according to the solution obtained by the last problem A1-M.

- **Step C: Flexibility index evaluation**

Step C-1: Solve the flexibility index problem (FI-M). The Flexibility Index (FI) and a new critical operating point are obtained using the active set strategy (ASS).

Step C-2: If FI is greater than 1, an optimal flexible heat exchanger network is obtained, stop and go to step D. Otherwise, set $P = P + 1$, add the last critical operating point to the multi-period formulation (new realizations of inlet temperatures and inlet flow rates) and return to step A-2.

- **Step D: Control structure design**

Step D-1: Obtain the steady-state gain matrices ($\mathbf{G}^p$ and $\mathbf{D}^p$) of the final optimal and flexible network with respect to inputs and perturbations in the nominal operating point (NP) and the critical points (CP).

Step D-2: Solve the control structure design problem. The control structure design is obtained by solving the model SSD-M for each operating point. This guarantees that the network operates satisfactorily at least in the operation points considered in synthesis stage.

3 Numerical Examples

Three case studies taken from the literature are presented in this section to illustrate the application of the different stages of the proposed strategy. Section 3.1 is focused on the optimization method and the outer-approximation strategy applied to the Synflex problem. Here, the relationships among the subproblems are shown. In Section 3.2, the solutions obtained at the synthesis stage for both the proposed global strategy and local optimization methods are compared. In turn, the solution of the control structure design problem obtained with the SSD strategy is presented in Section 3.3. The models FI-M, A1-M, A2-NLP, and A2-MIP have been formulated using GAMS v24.5. The proposed algorithmic method has been implemented in Matlab, and the Matlab-GAMS interface has been used to sequentially evaluate the required models (i.e., the multi-period design subproblems, the flexibility index model, and the control structure design formulation). The solvers CPLEX 12.6 and CONOPT 3 have been used to solve the subproblems A2-MIP and A2-NLP, respectively. In turn, BARON 15.9 has been employed both to evaluate the models A1-M and to solve the problems FI-M (MINLP). All models have been solved on an Intel Core i7 3.4 GHz machine with 8 GB of RAM. Three examples from the literature have been considered. The main data describing the HEN synthesis problems are presented in Tables 1 and 2. Examples 1 and 3 have been studied by Björk and Westerlund[13], and example 2 has been presented by Chen and Hung[40]. The case studies are analyzed taking into account increasing size and complexity, being the largest and more complex problem presented last. For every example, while case A considers changes of the inlet temperatures only, case B features not only inlet temperature but also inlet flow rate modifications. Examples 1-A, 1-B and 2-B are discussed in more detail.

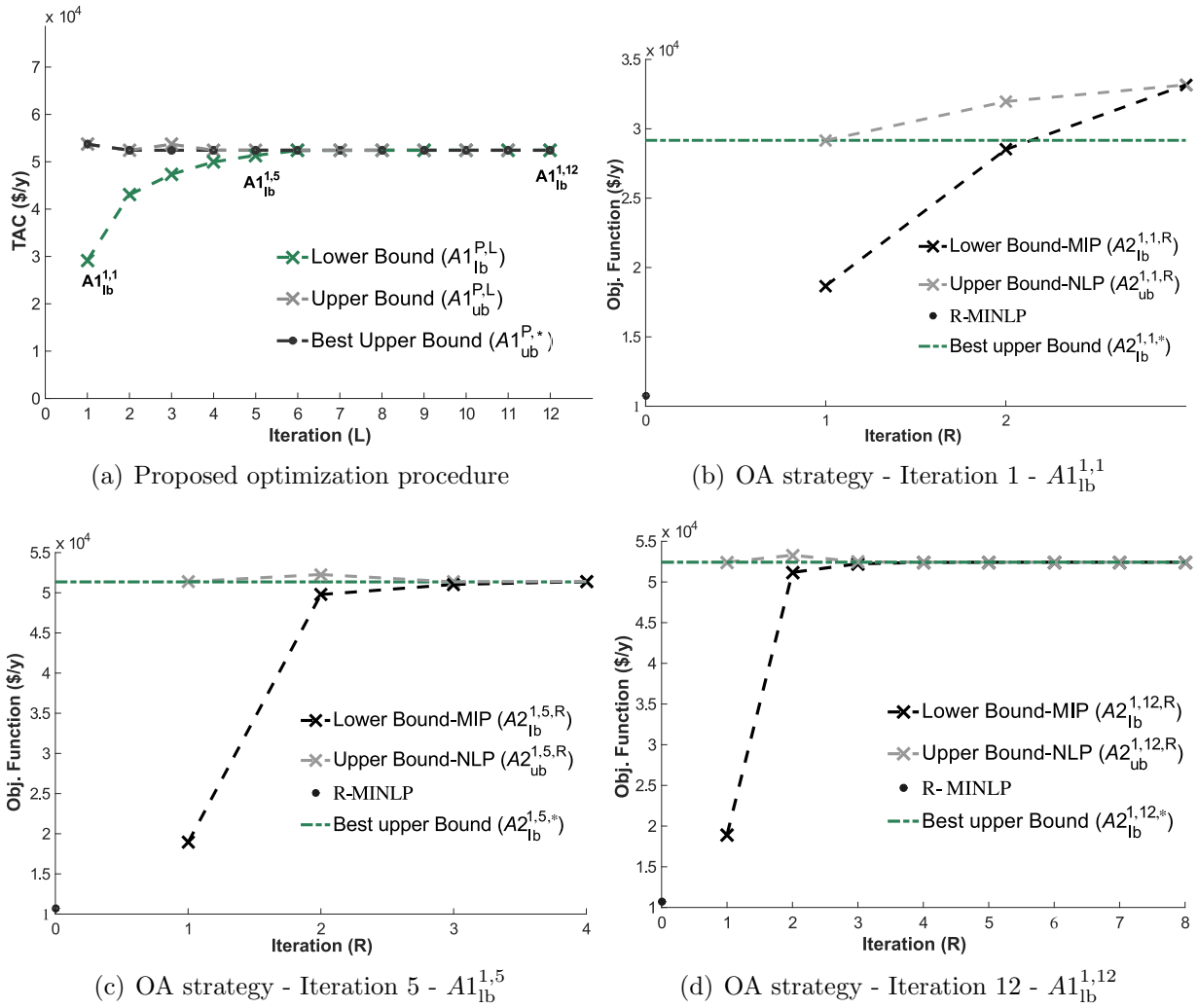

(a) Proposed optimization procedure

(b) OA strategy - Iteration 1 - $A1_{\mathrm{lb}}^{1,1}$

(c) OA strategy - Iteration 5 - $A1_{\mathrm{lb}}^{1,5}$

(d) OA strategy - Iteration 12 - $A1_{\mathrm{lb}}^{1,12}$

Figure 2: Proposed method using Outer-Approximation strategy – Example 1 – case A – period 1

3.1 Convergence Analysis of the Proposed Method

The purpose of this section is to show the convergence properties of the convexification strategy and the inner-outer optimization used to solve the proposed mixed-integer nonlinear multi-period design problem. The example 1, case A, involves one hot stream, two cold streams, and only disturbances in the inlet temperatures. For the nominal operating point (period 1) the objective value reported by Björk and Westerlund[13] is 52429 $\$y^{-1}$. Figure 2 illustrates the convergence of the proposed methodology for period $P = 1$.

The lower bound of model A1-M is obtained by convexifying the original problem to gen-

erate a relaxed formulation (A2-M). As presented in subsection 2.2.1, the relaxation applied is based on a piecewise linear approximation. On the one hand, by improving the approximation at each iteration (L), the new problem becomes a more accurate underestimation of the original problem. Thus, an increasing lower bound is obtained. The upper and lower bounds of the original problem ($A1^{1,L}_{\text{ub}}$ and $A1^{1,L}_{\text{lb}}$) are shown in Figure 2(a). At iteration 12, the final gap between the bounds is less than 1×10^{-4} and the best upper bound obtained ($A1^{1,*}_{\text{ub}}$) is 52428.65 \$y^{-1}.

On the other hand, in order to solve the subproblems A2-M at each iteration L, an outer-approximation strategy is used. This strategy is shown in Figures 2(b) to 2(d) for iterations $L = 1$, 5 and 12. For each subproblem A2-M, a sequence of successive lower and upper bounds ($A2^{P,L,R}_{\text{lb}}$ and $A2^{P,L,R}_{\text{ub}}$, respectively) are calculated by solving the models A2-MIP and A2-NLP at each iteration R. Figure 2(b) shows this sequence for $P = 1$ and $L = 1$, where the crossover between $A2^{1,1,R}_{\text{lb}}$ and $A2^{1,1,R}_{\text{ub}}$ can be observed at $R = 3$. As defined in the proposed method, the best upper bound ($A2^{1,1,*}_{\text{ub}} = 28507.25$ \$y^{-1}) is also the lower bound of the subproblem A1-M at iteration $L = 1$ ($A1^{1,1}_{\text{lb}} = A2^{1,1,*}_{\text{ub}}$). This can be seen by comparing the best upper bound in Fig. 2(b) with the lower bound at iteration $L = 1$ in Fig. 2(a). A similar observation is possible by considering the iterations 5 and 12 in Figures 2(c) and 2(d), respectively. In the general case, $A2^{P,L,*}_{\text{ub}} = A1^{P,L}_{\text{lb}}$ at each step L.

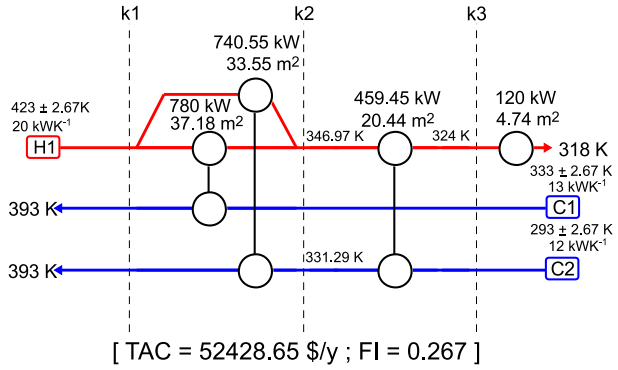

Figure 3: Optimal HEN structure for example 1 – case A – period 1

The final optimal configuration of the HEN at period $P = 1$ is shown in Figure 3. For this result, the flexibility index model (FI-M) is solved to obtain both the flexibility index

and a new critical point. If all the heat exchangers are used to control the network, the flexibility index is 0.267. Thus, a new critical point is added to the nominal condition, and the multi-period optimization problem is solved again by considering these two periods. In Table 4, the bounds $A1_{\text{lb}}^{2,L}$ and $A1_{\text{ub}}^{2,L}$ are reported for period $P = 2$. At iteration $L = 14$ the gap between $A1_{\text{ub}}^{2,L}$ and $A1_{\text{lb}}^{2,L}$ is less than 1×10^{-4} and the best upper bound ($A1_{\text{ub}}^{2,*}$) is 59766.57 \$y^{-1}. The new optimal configuration features a flexibility index of 2. Hence, the final optimal and flexible network has been found. Figure 4 presents the optimal and flexible HENs obtained at example 1 for both case A and case B. Recall that case B features not only inlet temperature but also inlet flow rate modifications. For this example the final objective value is 59630.55 \$y^{-1}, also with a flexibility index of 2. By comparing cases A and B it can be noted that final results obtained are different. This is because each case incorporates different critical points in the second period. The specific critical points added in each case are reported in Table 3.

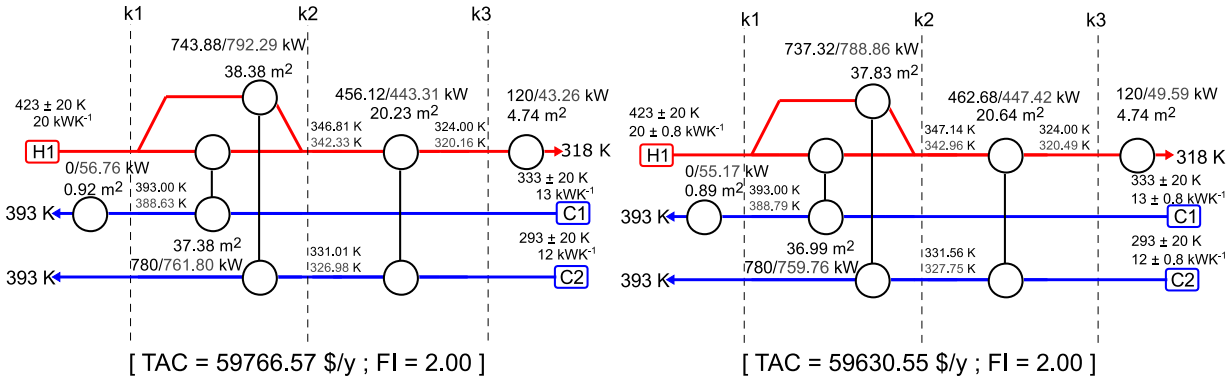

(a) Case A (b) Case B

Figure 4: Optimal HEN structures for example 1 – period 2

3.2 Comparison with Local Optimization Methods

The purpose of this section is to compare the quality of the Synflex problem solutions obtained with the proposed approach against those obtained with other local optimization methods. In this context, standard MINLP solvers that do not guarantee global optimality

are used to solve the non-convex model A1-M (i.e., without the convexification strategy). In particular, the solvers DICOPT, SBB and BONMIN are tested and compared with the proposed methodology.

Table 5 includes the objective function values for the global and best locally optimal solutions obtained for all the examples presented in Table 1 and Table 2. It can be observed that the local solutions reported by the solvers being tested have large variations compared with the solutions given by the proposed optimization strategy, particularly for Examples 2 and 3. Moreover, depending on the initial point, local optimization solvers (such as BONMIN or SBB) can even fail to find a feasible solution. This behavior is shown in Table 5 with a double asterisk (**) and is more frequent when multiple periods or large-scale problems are considered. In contrast, because of the convexification strategy applied, the outer-approximation obtains the best solutions for all the test cases being analyzed. The computing times for all the examples are reported in Table 6. For the proposed approach, more accurate solutions closer to the global optimum can be obtained at the expense of more CPU time. Recall that the stopping criterion of the proposed algorithm is the condition $|1 - A1_{\text{lb}}^{P,L}/A1_{\text{ub}}^{P,*}| \leq \mathcal{E}$. For all the examples, the value $\mathcal{E} = 1 \times 10^{-4}$ has been selected. A smaller $\mathcal{E}$ will allow more accurate solutions to be found. While the proposed strategy guarantees the optimality of the best solutions obtained, it should be noted that a large increase on the required CPU time can make it not suitable for medium/large scale problems.

In Figure 5, the best solutions found by the local optimization methods are compared with those of the proposed approach. The value 100% represents the global optimal objective for example 2 (cases A and B). It is clear from this figure that, if the convexity of the problem is not guaranteed, local optimization methods may get poor solutions which may differ considerably from the optimal value. In Figure 5, the solutions with the greatest deviations from their respective global solution are obtained by DICOPT.

For example 2, case B, the network configurations obtained with the proposed methodology at each iteration P are shown in Fig. 6. In the first iteration of the synthesis strategy,

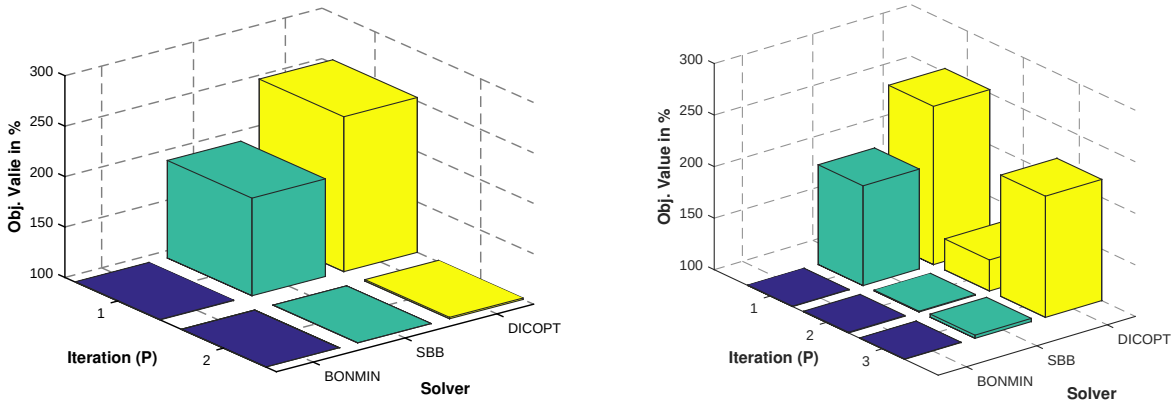

(a) Example 2, case A

(b) Example 2, case B

Figure 5: Comparison of optimal solutions (100%) with local solver solutions for model Synflex

Fig. 6(a), the best solution features an objective value of 30304.21 $\$y^{-1}$ and a flexibility index of 0.131. In the second iteration ($P = 2$), the nominal condition and the first critical point are considered to obtain a new flexible HEN, which is shown in Fig. 6(b). A heat exchanger is incorporated in this new configuration. Therefore, the objective value and the flexibility index increase to 31444.18 $\$y^{-1}$ and 0.636, respectively. However, the network still cannot handle the expected variations of the inlet disturbances. The optimal and flexible HEN is found in the third iteration of the synthesis strategy, Fig. 6(c), where the optimal objective value is 36540.41 $\$y^{-1}$ and the flexibility index is 1.713. It is important to note that a reasonable increase of the investment and operating cost, which corresponds to a higher TAC, is required to increase the flexibility index at each iteration.

3.3 Control Structure Design Results

The application of the control structure design (CSD) methodology is analyzed in this section. The problem 1, case B, where expected variations of the inlet temperatures and flow rates are simultaneously considered, is used to illustrate the proposed CSD approach. In section 3.1, the final flexible HEN obtained for this example has been shown in Fig. 4(b).

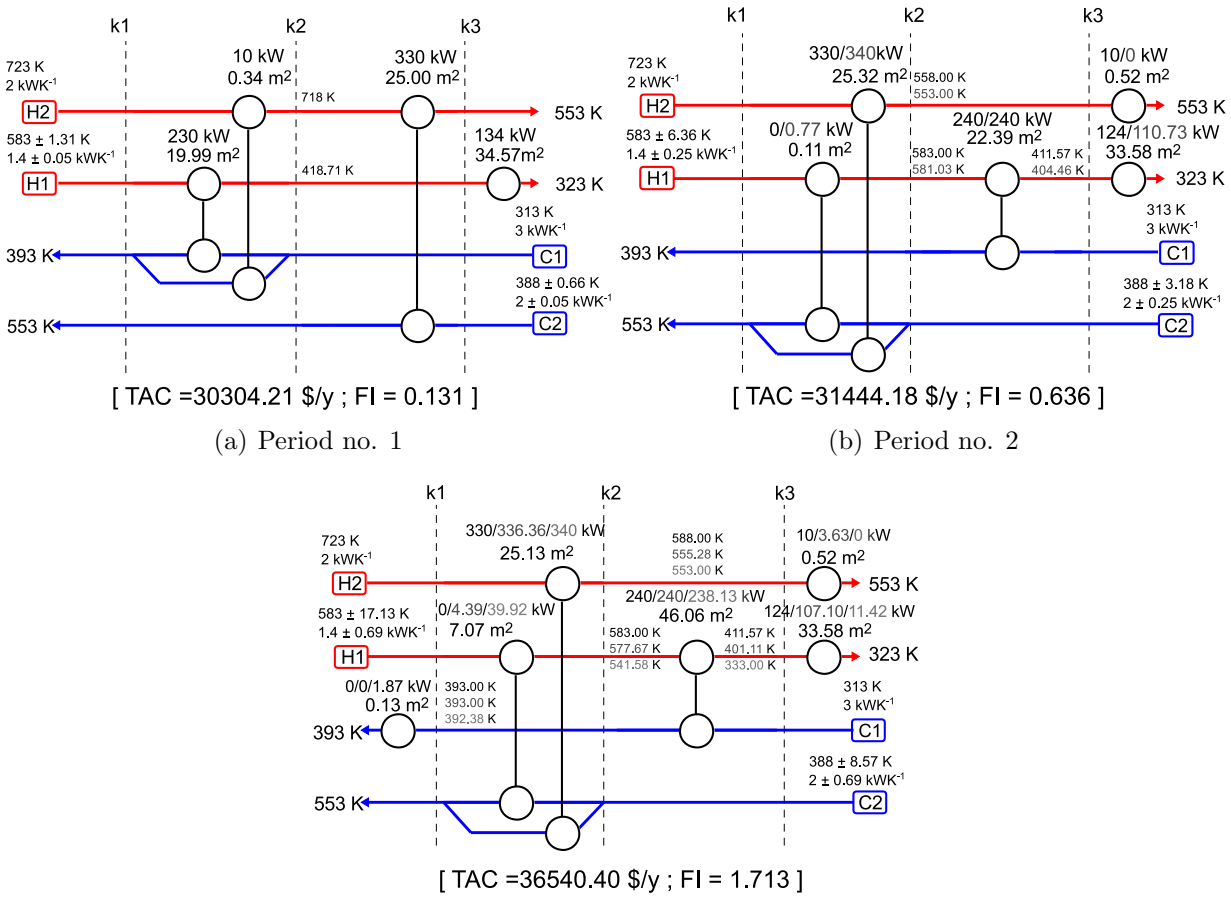

Figure 6: Optimal HEN structures for example 2 – case B

This HEN can operate under a range of inlet variations determined by its flexibility index. However, since the network structure is different for each design point, from the control perspective the steady-state gain of the system varies for each point. Indeed, depending on the disturbance amplitude and direction some equipment of the HEN are either turned on or turned off to handle these variations. In this context, the CSD method should be applied at least at each of these points. This fact is a contribution of this work with regards to Escobar et al.[21] where, paradoxically, the CSD is performed only at the nominal operating point.

The first step of the CSD methodology is to compute the steady-state gains for the flexible optimal HEN both at the nominal point and by considering the additional critical points. For problem 1, case B, the matrices $\mathbf{G}^p$ and $\mathbf{D}^p$ of the final flexible HEN at nominal

condition ($p = 1$) are:

$$\mathbf{G}^1 = \begin{bmatrix} 4.620 & 0 & 4.882 & -0.481 & 3.629 & 0 & 3.876 & -0.823 & -1.428 & 0 & 0 \\ -2.610 & 0 & 0 & 0 & -2.051 & 0 & 0 & 0 & 0 & 0 & 0 \\ 1.885 & 0 & -0.832 & -0.687 & 1.481 & 0 & -0.661 & -1.176 & 0 & 0 & 0 \end{bmatrix}$$

$$\mathbf{D}^1 = \begin{bmatrix} 0.458 & 1.179 & 0.762 & 51.578 & -11.581 & -25.899 \\ 0.667 & 0.333 & 0 & 5.395 & -8.347 & 0 \\ 0.859 & 0.481 & 0.231 & 16.979 & -2.835 & -15.675 \end{bmatrix}$$

and the steady-state gains of the HEN working at the second operation point ($p = 2$) are:

$$\mathbf{G}^2 = \begin{bmatrix} 4.946 & 0 & 4.636 & -0.465 & 3.643 & 0 & 3.878 & -0.786 & -0.552 & 0 & 0 \\ -2.639 & 0 & 0 & 0 & -1.944 & 0 & 0 & 0 & 0 & 0.885 & 0 \\ 1.836 & 0 & -1.059 & -0.606 & 1.352 & 0 & -0.886 & -1.023 & 0 & 0 & 0 \end{bmatrix}$$

$$\mathbf{D}^2 = \begin{bmatrix} 0.419 & 1.209 & 0.771 & 51.196 & -11.471 & -25.761 \\ 0.645 & 0.355 & 0 & 5.365 & -9.012 & 0 \\ 0.857 & 0.449 & 0.213 & 16.174 & -2.554 & -15.353 \end{bmatrix}$$

Moreover, the inputs, outputs, and disturbances are: $\mathbf{u} = [\mathrm{uh}_{111}, \mathrm{uh}_{112}, \mathrm{uh}_{121}, \mathrm{uh}_{122}, \mathrm{uc}_{111}, \mathrm{uc}_{112}, \mathrm{uc}_{121}, \mathrm{uc}_{122}, \mathrm{q}_1^{\mathrm{cu}}, \mathrm{q}_1^{\mathrm{hu}}, \mathrm{q}_2^{\mathrm{hu}}]^{\mathrm{T}}$, $\mathbf{y} = [\mathrm{Th}_1^{\mathrm{out}}, \mathrm{Tc}_1^{\mathrm{out}}, \mathrm{Tc}_2^{\mathrm{out}}]^{\mathrm{T}}$, and $\mathbf{d}^* = [\mathrm{Th}_1^{\mathrm{in}}, \mathrm{Tc}_1^{\mathrm{in}}, \mathrm{Tc}_2^{\mathrm{in}}, \mathrm{fh}_1^{\mathrm{in}}, \mathrm{fc}_1^{\mathrm{in}}, \mathrm{fc}_2^{\mathrm{in}}]^{\mathrm{T}}$, respectively. Based on these data, the SSD problem is solved to obtain the control structure for each operating point.

Figure 7 shows two different control structures for the HEN when working on two operating points (nominal point + critical point). The first control structure (CS1) is based on the paring $\mathrm{q}_1^{\mathrm{cu}}$ – $\mathrm{Th}_1^{\mathrm{out}}$, uh_{111} – $\mathrm{Tc}_1^{\mathrm{out}}$, and uc_{122} – $\mathrm{Tc}_2^{\mathrm{out}}$, and is feasible for a given region of the

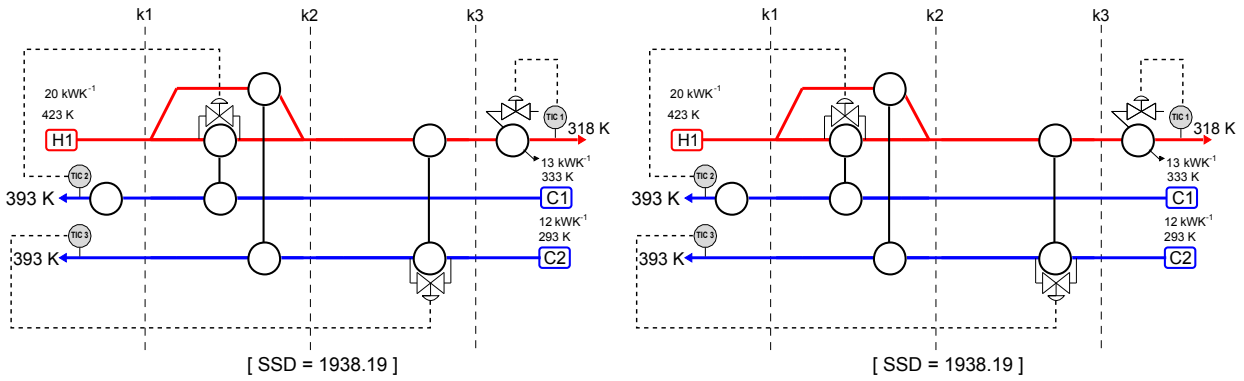

(a) Control structure no. 1 (CS1). (b) Control structure no. 2 (CS2).

Figure 7: Optimal control structures for the flexible HEN of example 1 – case B

perturbations. This control feasible region is inside of the feasible region determined by the first critical point, $|\mathbf{d}^*| \leq 0.216$. The steady-state gain matrix changes when the operation of the HEN moves from the nominal point towards the first critical point and, therefore, a second control structure (CS2) must be designed. On this critical direction, the hot utility exchange 1 must be turned on. Therefore, CS1 is reconfigured to CS2, which defines the following input-output pairing: uh_{111} – $\mathrm{Th}_1^{\mathrm{out}}$, $\mathrm{q}_1^{\mathrm{hu}}$ – $\mathrm{Tc}_1^{\mathrm{out}}$, and uc_{122} – $\mathrm{Tc}_2^{\mathrm{out}}$. This reconfiguration is required for certain directions when the perturbations leave the feasible region of CS1. In particular, CS2 is valid in the surroundings of the first critical point. Within this range, CS1 cannot operate the HEN because it cannot satisfy the energy requirement. While the hot utility exchanger should be turned on, CS1 does not have action on this variable. The fact that the hot utility exchanger is not running at the nominal operation point can be observed in the matrix G^1, which includes a zero column for this manipulated variable. It important to note that the flexibility index quantifies the maximum possible deviation allowed by the design without the control limitations. For this reason, a more detailed study is required to calculate the final feasible area of each control structure, i.e. to obtain the maximum possible deviation of the HEN working at closed loop. This detailed study is out of the scope of this work, and will be considered in future contributions. An additional result showing the dynamic behavior of temperature in the case when control reconfiguration is

needed has been included in the Supporting Information file.

In Tables 7, 8 and 9 the optimal control structures and the objective function values are shown for all the examples presented. In all cases the switching between alternative control structures can be implemented using override control based on PID controllers. Override control is a well-know methodology in industrial process control practice. Alternatively, advanced process control strategies such as MPC can be applied to handle all the control structures in a single layout.

4 Conclusions and Future Works

A new sequential methodology to obtain both the optimal design and the optimal control structure for flexible heat exchanger networks (HEN) is presented. The proposed approach determines both the HEN and the control structures able to operate it, within a given range of uncertain conditions (disturbances). The flexible HEN synthesis problem is handled by an iterative procedure where a sequence of multi-period formulations are solved. These multi-period models include non-convexities which are reformulated using a convexification technique before applying an outer-optimization strategy to obtain the optimal solutions. The proposed method guarantees that the optimal heat exchanger networks are obtained even when the flexibility is increased. In order to emphasize the importance of finding the optimal solution, the proposed global optimization strategy has been compared with alternative local optimization methods. The results clearly exemplify that local methods can obtain poor solutions with large deviations with respect to optimal value. Moreover, in some cases the local methods cannot find a feasible solution. In contrast, the convexification technique applied before solving the multi-period problems guarantees that the outer-approximation strategy obtains the optimal solutions. Besides, it is worth mentioning that the flexibility index increases when additional periods (i.e., critical operating points) are considered, producing a higher total annualized cost (TAC), which in turn is composed by reasonably higher

investment and operating costs.

An additional contribution of this work is the approach used at the control structure design (CSD) phase, which is based on the sum of squared deviations (SSD) index. The proposed CSD approach represents an advance when compared with previous contributions where the classical relative gain array (RGA) concept is applied only at the nominal operating point. In this context, an SSD-based control design formulation is proposed that systematizes (and combines in a single MIQP model) decisions such as the selection of controlled/manipulated variables and the input-output pairing. This formulation is solved for each period to obtain a valid control structure for each operating point. A case study is presented showing that the control structure designed for the nominal point cannot operate when the disturbances exceed the corresponding flexibility index. When this happens, the disturbance variations enforce some manipulated variables to be either active or turned off. A similar situation arises when the disturbances are higher than the flexibility index of any critical point. By using a reconfigurable control structure, the proposed approach allows the final flexible HEN to operate within a wider range of uncertainty conditions. However, a more detailed methodology is still required to determine and guarantee an appropriate final feasibility area for the controlled HEN.

In future work modifications of the synthesis problem, such as considering non-isothermal mixing and isothermal process streams, will be analyzed. Moreover, the optimization procedure will be improved by incorporating cuts, between consecutive iterations, to eliminate solutions of the approximate problem that exceed the objective value of the original problem on previous iterations. The aim of these cuts will be to improve the computational performance of the optimization strategy. Some preliminary results are shown in the Supporting Information file. Furthermore, the integration between synthesis and control will be further developed by considering alternative controller structures, such as decentralized, sparse, and full. Finally, the proposed methodology will be extended to retrofit the obtained HEN and the nominal bypass fraction based on analyzing the disturbance propagation in the network.

Acknowledgments

The authors thank the financial support of CIFASIS-CONICET, ANPCYT, UNR and UTN-FRRo from Argentina.

Nomenclature

Acronyms

AP/OA/ER: Augmented - Penalty - function / Outer - Approximation / Equality - Relaxation

BMINLP: Bilevel mixed-integer nonlinear programming

CSD: Control structure design

CVs: Controlled variables

CP: Critical points

FI: Flexibility index

HEN: Heat exchanger network

KKT: Karush-Kuhn-Tucker optimality conditions

RGA: Relative gain array

MINLP: Mixed-integer nonlinear programming

MILP: Mixed-integer linear programming

MIQP: Mixed-integer quadratic programming

MVs: Manipulated variables

NLP: Non-linear programming

NLE: Net load evaluation

NP: Nominal point

SSD: Sum of squared deviations

TAC: Total annal cost

TFM: Transfer function matrix

Sets and indices

$i \in I = \{1, \ldots, \mathrm{N_H}\}$: hot streams

I': relevant equality constraints selected from eqs. (1b)

$j \in J = \{1, \ldots, \mathrm{N_C}\}$: cold streams

J': relevant inequality constraints selected from eqs. (1c)

$k \in K = \{1, \ldots, \mathrm{N_T}\}$: stages

$l = 1, \ldots, L$: gridpoints of the piece-wise approximation

L: iteration of the convexification strategy

R: iteration of the outer-approximation strategy

$p = 1, \ldots, P$: periods

$\sigma = 1, \ldots,$ M': set point changes of controlled output variables

P: iteration of the multi-period synthesis strategy

$\omega = 1, \ldots,$ D': perturbations

$\ell = 1, \ldots,$ N': manipulated variables

$\nu = 1, \ldots,$ M': controlled output variables

Continuous variables

$A1^P$: optimal economic objective function value at iteration P

$A1^{P,L}_{\text{ub}}$: upper bound of the model A1-M at iterations P and L.

$A1^{P,L}_{\text{lb}}$: lower bound of the model A1-M at iterations P and L.

$A1^{P,*}_{\text{ub}}$: best upper bound of the model A1-M at iteration P.

$A2^{P,L}$: economic objective function value of model A2-M at iterations P and L

$A2^{P,L,R}_{\text{ub}}$: upper bound of the model A2-M at iterations P, L, and R

$A2^{P,L,R}_{\text{lb}}$: lower bound of the model A2-M at iterations P, L, and R

$A2^{P,L,*}_{\text{ub}}$: best upper bound of the model A2-M at iterations P and L

a, a_{cu}, and a_{hu} : areas of heat exchangers, cold utility exchangers, and hot utility exchangers, respectively, raised to the power of β

$\mathbf{d}$: design variables

$\mathbf{dz}_p$: variables used to convexify the signomial terms present in model A1-M

FI^P: flexibility index at iteration P

q, q_{cu}, and q_{hu}: heats associated to heat exchangers, cold utility exchangers, and hot utility exchangers, respectively

SSD^p: sum of squared deviations index for the optimal HEN working at the operating point p

$s_{j'}$: slack variables of the inequality j'

$\mathbf{u}$: input vector

$\mathbf{u}_{\text{s}}$: MVs vector

$\mathbf{u}_{\text{r}}$: non-selected MVs vector

$\mathbf{u}^{\text{c}p}_{\sigma} = [u^{\text{c}p}_{\ell,\sigma}]$: input response vector for the σ-th set-point change at period p

$\mathbf{u}^{\text{d}p}_{\omega} = [u^{\text{d}p}_{\ell,\omega}]$: input response vector for the ω-th disturbance effect at period p

$\mathbf{x}_{\text{H}}$: continuous variables of the model A1-M

$\mathbf{x}_{\text{F}}$: continuous variables of the model FI-M

$\mathbf{x}_{\text{C}}$: continuous variables of the model A2-M

$\mathbf{x}_p$: dependent (state) variables

$\mathbf{y}$: output vector

$\mathbf{y}_{\text{s}}$: CVs vector

$\mathbf{y}^{\text{r}p} = [y^{\text{r}p}_{\sigma,\ell}]$: RGA matrix at period p

$\mathbf{z}_p$: independent (manipulated) variables

Δt: temperature difference between cold and hot stream

δ: fraction of the maximum expected disturbances

$\lambda_{j'}$: lagrange multipliers associated to the inequality constraint j'.

$\mu_{i'}$: lagrange multipliers associated to the equality constraint i'

$\mu_{r,\kappa}$: KKT multipliers associated with the κ-th inequality constraints g_κ and obtained from the NLP problem solved at iteration r

$\boldsymbol{s}_r$: slack variables

$\boldsymbol{\theta}^*_{\mathrm{P}+1}$: critical point of model FI-M.

$\boldsymbol{\Gamma}$: direction that $\boldsymbol{\theta}^*_{\mathrm{P}+1}$ deviates from the nominal point

Binary Variables

$\mathbf{w}_p$: interval selection of piecewise linear-approximation

$\mathbf{y}_{\mathrm{H}}$: binary variables of the model A1-M

$\mathbf{y}_{\mathrm{F}}$: binary variables of the model FI-M

$\mathbf{y}_{\mathrm{C}}$: binary variables of the model A2-M

$\mathbf{y}$: existence of heat exchangers and utility exchangers

$\mathbf{y}'_p$: operation of heat exchangers and utility exchangers

$y^{\mathrm{F}}_{j'}$: activation of the inequality constraint j'

$\mathbf{z}^{\mathrm{I}p} = [z^{\mathrm{I}p}_\ell]$: MVs selection for operating point p

$\mathbf{z}^{\mathrm{nd}p} = [z^{\mathrm{nd}p}_{\nu,\ell}]$: binary matrix for decentralized control structure selection of operating point p.

Parameters

$\mathbf{D}_{\mathrm{s}}$: disturbance TFM for CVs

$\mathbf{d}^*$: disturbance vector

$\mathbf{D}^p = [d^p_{\nu,\omega}]$: HEN disturbance TFM at operating point p

$\mathbf{D}$: disturbance TFM

$\mathbf{G}$: process TFM

$\mathbf{G}_{\mathrm{s}}$: process TFM for CVs

$\mathbf{G}^p = [g^p_{\nu,\ell}]$: HEN TFM for CVs at operating point p

$\boldsymbol{\theta}_p$: operating point at period p

$\boldsymbol{\Phi}^P$: HEN design obtained at iteration P

$\mathrm{M_F}$: upper bound for the slack variables $s_{j'}$

$\mathrm{M_S}$: big-M

n_z: number of control variables selected

$\mathbf{v}_\sigma$ and $\mathbf{v}_\omega$: unit vectors of directions σ and ω, respectively

$\mathbf{wk}_r$: weights of the slack variables $\boldsymbol{s}_r$

δ_1/δ_2: lower/upper bound for RGA pairing entries

$\Delta\boldsymbol{\theta}^{+}/\Delta\boldsymbol{\theta}^{-}$: maximum positive/negative expected disturbances

$\phi_{\nu,\sigma}$: (ν,σ)-th entry of the identity matrix

Supporting Information

This material is available free of charge via the Internet at http://pubs.acs.org/.

A detailed description of the A1-M, A2-M, and A2-MIP models are discussed in the supporting information file.

References

(1) Mathisen, K. W. Integrated design and control of heat exchanger networks. *Ph.D. Thesis. Trondheim University. NTH Norway* **1994**,

(2) Papoulias, S. A.; Grossmann, I. E. A structural optimization approach in process synthesis II. Heat recovery networks. *Computers & Chemical Engineering* **1983**, *7*, 707.

(3) Linnhoff, B.; Hindmarsh, E. The pinch design method for heat exchanger networks. *Chemical Engineering Science* **1983**, *38*, 745–763.

(4) Floudas, C. A.; Ciric, A. R.; Grossmann, I. E. Automatic synthesis of optimum heat exchanger network configurations. *AIChE Journal* **1986**, *32*, 276–290.

(5) Yee, T. F.; Grossmann, I. E. Simultaneous optimization models for heat integrations II. Heat exchanger network synthesis. *Computers & Chemical Engineering* **1990**, *14*, 1165.

(6) Ponce-Ortega, J. M.; Jiménez-Gutiérrez, A.; Grossmann, I. E. Optimal synthesis of heat exchanger networks involving isothermal process streams. *Computers & Chemical Engineering* **2008**, *32*, 1918–1942.

(7) Grossmann, I. E.; Yeomans, H.; Kravanja, Z. A rigorous disjunctive optimization model for simultaneous flowsheet optimization and heat integration. *Computers & Chemical Engineering* **1998**, *22*, 157–164.

(8) Onishi, V. C.; Ravagnani, M. A. S.; Caballero, J. A. Simultaneous synthesis of work exchange networks with heat integration. *Computers & Chemical Engineering* **2014**, *112*, 87–107.

(9) Serna-Gonzalez, M.; Ponce-Ortega, J. M.; Jiménez-Gutiérrez, A. Two-level optimization algorithm for heat exchanger networks including pressure drop considerations. *Engineering Chemistry Research* **2004**, *43*, 6766–6773.

(10) Mizutani, F. T.; Pessoa, F. L. P.; Queiroz, E. M.; Hauan, S.; Grossmann, I. E. Mathematical programming model for heat-exchanger network synthesis including detailed heat-exchanger designs 2. Networks synthesis. *Industrial and Engineering Chemistry Research* **2003**, *42*, 4019–4027.

(11) Frausto-Hernandez, S.; Rico-Ramirez, V.; Jiménez-Gutiérrez, A.; Hernandez-Castro, S. MINLP synthesis of heat exchanger networks considering pressure drop effects. *Computers & Chemical Engineering* **2003**, *27*, 1143–1152.

(12) Furman, K. C.; Sahinidis, N. A critical review and annotated bibliography for heat exchanger network synthesis in the 20th century. *Industrial and Engineering Chemistry Research* **2002**, *41*, 2335–2370.

(13) Björk, K. M.; Westerlund, T. Global optimization of heat exchanger network synthesis problems with and without the isothermal mixing assumption. *Computers & Chemical Engineering* **2002**, *26*, 1581–1593.

(14) Braccia, L.; Degliuomini, L. N.; Luppi, P.; Basualdo, M. S. Global Optimization for Flexible Heat Exchanger Network Synthesis of Chemical Plant . *24th European Symposium on Computer Aided Process Engineering – ESCAPE 24*. **2014**, *33*, 199–204.

(15) Bergamini, M. L.; Grossmann, I. E.; Scenna, N.; Aguirre, P. An improved piecewise outer approximation algorithm for the global optimization of MINLP models involving concave and bilinear terms. *Computers & Chemical Engineering* **2008**, *32*, 477–493.

(16) Zamora, J. M.; Grossmann, I. E. A branch and contract algorithm for problems with concave univariate, bilinear and linear fractional terms. *Journal of Global Optimization* **1999**, *14*, 2173.

(17) Adjiman, C. S.; Androulakis, I. P.; Floudas, C. A. Global optimization of mixed-integer nonlinear problems. *AIChE Journal* **2000**, *46*, 1769–1797.

(18) Aaltola, J. Simultaneous Synthesis of Flexible Heat Exchanger Networks. *Thesis, Department of Mechanical Engineering, Helsinki University of Technology, Finland.* **2002**,

(19) Chen, L. C.; Hung, P. S. Simultaneous synthesis of flexible heat-exchange networks with uncertain source-stream temperatures and flow rates. *Industrial & Engineering Chemistry Research* **2004**, *43*, 5916–5928.

(20) Verheyen, W.; Zhang, N. Design of flexible heat exchanger network for multi-period operation. *Chemical Engineering Science* **2006**, *61*, 7730–7753.

(21) Escobar, M.; Trierweiler, J. O.; Grossmann, I. E. Simultaneous synthesis of heat exchanger networks with operability considerations: Flexibility and controllability. *Computers & Chemical Engineering* **2013**, *55*, 158–180.

(22) Morari, M. Effect of Design on the Controllability of Chemical Plants. *Proc. IFAC Workshop on Interactions Between Process Design and Process Control, London* **1992**, *44*, 3.

(23) Calandranis, J.; Stephanopoulos, G. A Structural Approach to the Design of Control Systems in Heat Exchanger Networks. *Computers & Chemical Engineering* **1988**, *12*, 651.

(24) Aguilera, N.; Marchetti, J. L. Optimizing and Controlling the Operation of Heat-Exchanger Networks. *AIChE Journal* **1988**, *44*, 1090.

(25) Mathisen, K. W.; Skogestad, S.; Wolff, E. A. Controllability of Heat Exchanger Networks. *AIChE Meeting, Los Angeles, CA* **1991**,

(26) Mathisen, K. W.; Skogestad, S.; Gundersen, T. Optimal Bypass Placement in Heat Exchanger Networks. *AIChE Meeting, New Orleans, LA* **1992**,

(27) Papalexandri, K. P.; Pistikopoulos, E. N. A Multiperiod MINLP model for the Synthesis of Flexible Heat and Mass Exchange Network. *Computers & Chemical Engineering* **1994**, *18*, 1125.

(28) Papalexandri, K. P.; Pistikopoulos, E. N. Synthesis and Retrofit Design of Operable Heat Exchanger Network: 1. Flexiblility and Structural Controllability Aspects. *Industrial and Engineering Chemistry Research* **1994**, *33*, 1718.

(29) Yang, Y. H.; Lou, H. H.; Huang, Y. L. Steady-State Disturbance Propagation Modeling of Heat Integrated Distillation Process. *Transactions of the Institution of Chemical Engineers* **2000**, *Part A, 78*, 245.

(30) Yang, Q. Z.; Yang, Y. H.; Huang, Y. L. Cost-Effective Bypass Design of Highly Controllable Heat-Exchanger Networks. *AIChE Journal* **2001**, *47*, 2253–2276.

(31) Braccia, L.; García, M.; Luppi, P.; Basualdo, M. S. Synthesis of Flexible Heat Exchanger Networks Integrated with Reconfigurable Control Design. *12th International Symposium on Process Systems Engineering and 25th European Symposium on Computer Aided Process Engineering.* **2015**, *37*, 1421–1426.

(32) Luppi, P.; Outbib, R.; Basualdo, M. S. Nominal controller design based on decentralized integral controllability in the framework of reconfigurable fault-tolerant structures. *Industrial and Engineering Chemistry Research* **2015**, *54*, 1301–1312.

(33) Viswanathan, J.; Grossmann, I. E. A combined penalty function outer-approximation method minlp optimization. *Computers and Chemical Engineering.* **1990**, *14*, 769–782.

(34) Paterson, W. R. A replacement for the logarithmic mean. *Chemical Engineering and Sciences* **1984**, *39*, 1635.

(35) Swaney, R. E.; Grossmann, I. E. An index for operational flexibility in chemical process design – Part I: Formulation and theory. *AIChE Journal* **1985**, *31*, 631–630.

(36) Grossmann, I. E.; Floudas, C. A. Active constraint strategy for flexibility analysis in chemical processes. *Computers & Chemical Engineering* **1987**, *11*, 675–693.

(37) Braccia, L.; Marchetti, P.; Luppi, P.; Zumoffen, D. Multivariable control structure design based on mixed-integer quadratic programming. *Industrial & Engineering Chemical Research* **2017**, *56*, 11228–11244.

(38) Zumoffen, D. Plant-wide control design based on steady-state combined indexes. *ISA Transactions.* **2016**, *60*, 191–205.

(39) Zumoffen, D.; Basualdo, M. Improvements on multiloop control design via net load evaluation. *Computers and Chemical Engineering.* **2013**, *50*, 54–70.

(40) Chen, L. C.; Hung, P. S. Synthesis of flexible heat exchange networks and mass exchange networks. *Computers & Chemical Engineering* **2007**, *31*, 1619–1632.

Table 1: Problem data for the examples

Stream	$T_{in} \pm \Delta\theta$ [K]	T_{out} [K]	Heat transfer coefficient [$kW\,K^{-1}m^{-2}$]	$F_{in} \pm \Delta\theta$ [$kW\ K^{-1}$]
Example 1				
Case A				
Hot 1	423 ± 10	318	2	20
Cold 1	333 ± 10	393	2	13
Cold 2	293 ± 10	393	2	12
Hu	473	473	1	
Cu	278	288	1	
Case B				
Hot 1	423 ± 10	318	2	20 ± 0.4
Cold 1	333 ± 10	393	2	13 ± 0.4
Cold 2	293 ± 10	393	2	12 ± 0.4
Hu	473	473	1	
Cu	278	288	1	
Cost of heat exchanger [$\$y^{-1}$] $= 4000 + 560 \times \text{area}^{0.8}$,				
Cost of utility exchanger [$\$y^{-1}$] $= 4000 + 700 \times \text{area}^{0.8}$, Cost of Cooling utility [$\$kW^{-1}y^{-1}$] $= 20$,				
Cost of Heating utility [$\$kW^{-1}y^{-1}$] $= 80$.				
Case A, optimal sol. period 1: 52428.65 $\$y^{-1}$, FI: 0.267; period 2: 59766.56 $\$y^{-1}$, FI: 2.				
Case B, optimal sol. period 1: 52428.65 $\$y^{-1}$, FI: 0.216; period 2: 59630.55 $\$y^{-1}$, FI: 2.				
Example 2				
Case A				
Hot 1	583 ± 10	323	0.16	1.4
Hot 2	723 ± 10	553	0.16	2.0
Cold 1	313 ± 10	393	0.16	3.0
Cold 2	388 ± 10	553	0.16	2.0
Hu	573	573	0.16	
Cu	303	323	0.16	
Case B				
Hot 1	583 ± 10	323	0.16	1.4 ± 0.4
Hot 2	723	553	0.16	2.0
Cold 1	313	393	0.16	3.0
Cold 2	388 ± 5	553	0.16	2.0 ± 0.4
Hu	573	573	0.16	
Cu	303	323	0.16	
Cost of heat exchanger [$\$y^{-1}$] $= 1100 + 866.60 \times \text{area}^{0.6}$,				
Cost of utility exchanger [$\$y^{-1}$] $= 1100 + 866.60 \times \text{area}^{0.6}$, Cost of Cooling utility [$\$kW^{-1}y^{-1}$] $= 52.09$,				
Cost of Heating utility [$\$kW^{-1}y^{-1}$] $= 148.28$.				
Case A, optimal sol. period 1: 30304.21 $\$y^{-1}$, FI: 0.250; period 2: 31589.42 $\$y^{-1}$, FI: 1.429.				
Case B, optimal sol. period 1: 30304.21 $\$y^{-1}$, FI: 0.131; period 2: 31444.18 $\$y^{-1}$, FI: 0.636;				
period 3: 36540.41 $\$y^{-1}$, FI: 1.713.				

Table 2: Problem data for the examples (cont.)

Stream	$T_{in} \pm \Delta\theta$ [K]	T_{out} [K]	Heat transfer coefficient [kW K^{-1}m^{-2}]	$F_{in} \pm \Delta\theta$ [kW K^{-1}]
Example 3				
Case A				
Hot 1	180 ± 10	75	2	30
Hot 2	240 ± 10	60	2	40
Cold 1	40 ± 2	230	1.5	20
Cold 2	120 ± 2	260	1.5	15
Cold 3	40 ± 2	130	2	25
Cold 4	80 ± 2	190	2	20
Hu	325	325	1	
Cu	25	40	2	
Case B				
Hot 1	180 ± 10	75	2	30 ± 1.5
Hot 2	240 ± 10	60	2	40 ± 1.5
Cold 1	40 ± 5	230	1.5	20 ± 2
Cold 2	120 ± 2.5	260	1.5	15 ± 0.4
Cold 3	40 ± 2.5	130	2	25 ± 0.4
Cold 4	80 ± 10	190	2	20 ± 2
Hu	325	325	1	
Cu	25	40	2	

Cost of heat exchanger [\$y^{-1}] $= 8000 + 50 \times \text{area}^{0.75}$,
Cost of utility exchanger [\$y^{-1}] $= 8000 + 50 \times \text{area}^{0.75}$, Cost of Cooling utility [\$kW^{-1}y^{-1}] $= 20$,
Cost of Heating utility [\$kW^{-1}y^{-1}] $= 120$.
Case A, optimal sol. period 1: 169064.44 \$y^{-1}, FI: 0; period 2: 177328.89 \$y^{-1}, FI: 2.566.
Case B, optimal sol. period 1: 169064.44 \$y^{-1}, FI: 0; period 2: 177793.82 \$y^{-1}, FI: 1.543.

Table 3: Example 1 – Critical point considered in the second period

Case	$Thin_1^2$ [K]	$Fhin_1^2$ [kW K^{-1}]	$Tcin_1^2$ [K]	$Fcin_1^2$ [kW K^{-1}]	$Tcin_2^2$ [K]	$Fcin_2^2$ [kW K^{-1}]
A	420.03	20.00	330.03	13.00	290.03	12.00
B	420.75	19.91	330.75	13.09	290.75	12.09

Table 4: Proposed Optimization Method – Problem 1 – case A – period 2

Iteration $[L]$	$A1_{\text{lb}}^{2,L}$	$A1_{\text{ub}}^{2,L}$	Gap [%]
1	31461.57	63876.68*	1.03×10^{2}
2	49276.74	60055.83*	2.19×10^{1}
3	51545.38	62516.69	1.65×10^{1}
4	56746.96	59780.04*	0.53×10^{1}
5	58366.89	59958.93	0.24×10^{1}
6	59624.37	59800.39	2.61×10^{-1}
7	59720.37	59772.05*	8.65×10^{-2}
8	59752.49	59767.42*	2.49×10^{-2}
9	59764.49	59766.94*	4.08×10^{-3}
10	59765.91	59767.03	1.72×10^{-3}
11	59766.25	59766.67*	6.97×10^{-4}
12	59766.49	59766.58*	1.65×10^{-4}
13	59766.52	59766.71	1.13×10^{-4}
14	59766.54	59766.57*	5.03×10^{-5}

* Best upper bound $A1_{\text{ub}}^{P,*}$, Gap $= 100\left[1 - A1_{\text{lb}}^{P,L}/A1_{\text{ub}}^{P,*}\right]$

Table 5: Objective function [\$y^{-1}] for Synflex – Local solvers vs Proposed method

		Example 1		Example 2		Example 3	
	P	A	B	A	B	A	B
DICOPT	1	52428.65	52428.65	76830.63	76830.63	169137.45	169137.45
	2	59766.56	59630.55	32046.59	40905.79	177424.36	177869.12
	3				79498.09		
BONMIN	1	52428.65	52428.65	30437.95	30437.95	185118.02	185118.02
	2	59766.56	59630.55	31589.42	31659.48	**	**
	3				36673.32		
SBB	1	52428.65	52428.65	59635.17	59635.17	579366.18	579366.18
	2	59766.89	59630.88	31604.96	31674.63	**	**
	3				37671.05		
Proposed Method	1	52428.65	52428.65	30304.21	30304.21	169064.43	169064.43
	2	59766.57	59630.55	31589.42	31444.18	177328.89	177793.82
	3				36540.40		

** No feasible solution found

Table 6: Optimization times [s] for Synflex – Local Solvers vs Proposed method

		Example 1		Example 2		Example 3	
	P	A	B	A	B	A	B
DICOPT	1	0.11	0.11	0.38	0.38	4.87	4.87
	2	0.28	0.23	0.27	0.26	66.25	153.69
	3				0.26		
BONMIN	1	3.34	3.34	16.38	16.38	2796.05	2796.05
	2	10.22	9.58	305.14	66.63	**	**
	3				757.35		
SBB	1	0.19	0.19	0.29	0.29	80.36	80.36
	2	1.17	1.14	4.60	2.18	**	**
	3				4.67		
Proposed Method	1	5.63	5.63	54.96	54.96	359.28	359.28
	2	212.38	107.25	751.73	557.82	20322.92	18122.22
	3				1005.00		

Table 7: Alternative decentralized control structures for Example 1

Example 1				
	Case A		Case B	
	CS1	CS2	CS1	CS2
Pairings	Th_1^{out} – fcu_1	Th_1^{out} – uh_{111}	Th_1^{out} – fcu_1	Th_1^{out} – uh_{111}
	Tc_1^{out} – uh_{111}	Tc_1^{out} – fhu_1	Tc_1^{out} – uh_{111}	Tc_1^{out} – fhu_1
	Tc_2^{out} – uc_{122}	Tc_2^{out} – uc_{122}	Tc_2^{out} – uc_{122}	Tc_2^{out} – uc_{122}
SSD	1962.42	2117.34	1938.19	2205.41

Table 8: Alternative decentralized control structures for Example 2

Example 2					
	Case A		Case B		
	CS1	CS2	CS1	CS2	CS3
Pairings	Th_1^{out} – fcu_1	Th_1^{out} – fcu_1	Th_1^{out} – fcu_1	Th_1^{out} – fcu_1	Th_1^{out} – fcu_1
	Th_2^{out} – fcu_2	Th_2^{out} – uc_{221}	Th_2^{out} – fcu_2	Th_2^{out} – fcu_2	Th_2^{out} – uh_{221}
	Tc_1^{out} – uh_{112}	Tc_1^{out} – uh_{112}	Tc_1^{out} – uh_{112}	Tc_1^{out} – uh_{112}	Tc_1^{out} – uh_{112}
	Tc_2^{out} – uh_{221}	Tc_2^{out} – uc_{121}	Tc_2^{out} – uh_{221}	Tc_2^{out} – uc_{221}	Tc_2^{out} – uc_{121}
SSD	62.70	127710.85	52.90	60.32	593.60

Table 9: Alternative decentralized control structures for Example 3

Example 3				
	Case A		Case B	
	CS1	CS2	CS1	CS2
Pairings	Th_1^{out} – uc_{134}	Th_1^{out} – uc_{134}	Th_1^{out} – uc_{134}	Th_1^{out} – uc_{134}
	Th_2^{out} – fcu_2	Th_2^{out} – fcu_2	Th_2^{out} – uh_{242}	Th_2^{out} – uh_{242}
	Tc_1^{out} – uc_{212}	Tc_1^{out} – uc_{212}	Tc_1^{out} – uh_{212}	Tc_1^{out} – uh_{212}
	Tc_2^{out} – fhu_2	Tc_2^{out} – fhu_2	Tc_2^{out} – fhu_2	Tc_2^{out} – fhu_2
	Tc_3^{out} – uc_{122}	Tc_3^{out} – uc_{122}	Tc_3^{out} – uc_{122}	Tc_3^{out} – uc_{122}
	Tc_4^{out} – uh_{211}	Tc_4^{out} – uh_{211}	Tc_4^{out} – uh_{211}	Tc_4^{out} – uh_{211}
SSD	13355.08	13359.48	2057.62	2070.03

TOC Graphic

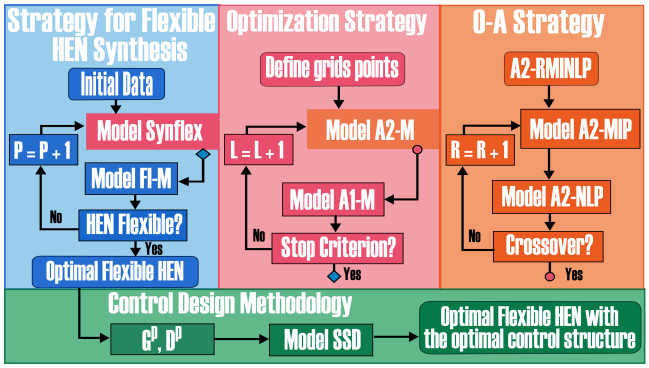
Strategy for Flexible HEN Synthesis
Initial Data
Model Synflex
P = P + 1
Model FI-M
No
HEN Flexible?
Yes
Optimal Flexible HEN
Optimization Strategy
Define grids points
Model A2-M
L = L + 1
Model A1-M
No
Stop Criterion?
Yes
O-A Strategy
A2-RMINLP
Model A2-MIP
R = R + 1
Model A2-NLP
No
Crossover?
Yes
Control Design Methodology
C^D, D^D
Model SSD
Optimal Flexible HEN with the optimal control structure